Design and Analysis of Stand-alone Agrivoltaic System. Case Study on Aysit Kebele, Afar Region

Hassen Mohammed Adem

A Thesis Submitted to

The department of Electrical Power and Control Engineering

School of Electrical Engineering and Computing

Presented in Partial Fulfillment of the Requirement for the Degree of Master's in Electrical Power and Control Engineering (Power System Engineering)

Office of Graduate Studies

Adama Science and Technology University

September 16, 2022

Adama, Ethiopia

Design and Analysis of Stand-alone Agrivoltaic System. Case Study on Aysit Kebele, Afar Region

Hassen Mohammed Adem

Advisor: Tefera Terefe (PhD)

A Thesis Submitted to

The department of Electrical Power and Control Engineering

School of Electrical Engineering and Computing

Presented in Partial Fulfillment of the Requirement for the Degree of Master's in Electrical Power and Control Engineering (Power System Engineering)

Office of Graduate Studies

Adama Science and Technology University

September 16, 2022

Adama, Ethiopia

Approval Page

I, the advisors of the thesis entitled "Design and Analysis of Stand-alone Agrivoltaic System. Case Study on Aysit Kebele, Afar Region" and developed by Hassen Mohammed Adem, hereby certify that the recommendation and suggestions made by the board of examiners are appropriately incorporated into the final version of the thesis.

Dr. Tefera T. Y. (Assistant Professor)	___________	09/15/2022
Major Advisor	Signature	Date

We, the undersigned, members of the Board of Examiners of the thesis by Hassen Mohammed Adem have read and evaluated the thesis entitled "Design and Analysis of Stand-alone Agrivoltaic System. Case Study on Aysit Kebele, Afar Region" and examined the candidate during open defense. This is, therefore, to certify that the thesis is accepted for partial fulfillment of the requirement of the degree of Master of Science in Electrical Power and Control Engineering (Power System Engineering)

______________________	__________	____________
Chairperson	Signature	Date
______________________	__________	____________
Internal Examiner	Signature	Date
______________________	__________	____________
External Examiner	Signature	Date

Finally, approval and acceptance of the thesis is contingent upon submission of its final copy to the Office of Postgraduate Studies (OPGS) through the Department Graduate Council (DGC) and School Graduate Committee (SGC).

______________________	__________	____________
Department Head	Signature	Date
______________________	__________	____________
School Dean	Signature	Date
______________________	__________	____________
Office of Postgraduate Studies, Dean	Signature	Date

Declaration

I hereby declare that this Master Thesis entitled "Design and Analysis of Stand-alone Agrivoltaic System. Case Study on Aysit Kebele, Afar Region" is my original work. That is, it has not been submitted for the award of any academic degree, diploma or certificate in any other university. All sources of materials that are used for this thesis have been duly acknowledged through citation

Hassen Mohammed	_______________	09/16/2022
Name of the student	Signature	Date

Recommendation

I, the advisor(s) of this thesis, hereby certify that I have read the revised version of the thesis entitled "Design and Analysis of Stand-alone Agrivoltaic System. Case Study on Aysit Kebele, Afar Region" prepared under my guidance by Hassen Mohammed Adem submitted in partial fulfillment of the requirements for the degree of Mater's of Science in Electrical Power and Control Engineering (Power System Engineering).

Therefore, I recommend the submission of revised version of the thesis to the department following the applicable procedures.

Dr. Tefera T. Y. (Assistant Professor)	__________	09/15/2022
Major Advisor	Signature	Date

Acknowledgements

Primarily I would like to express my sincere gratitude to Allah. This paper and the research behind it would not have been possible without the exceptional support of my Advisor, Dr. Tefera. His enthusiasm, knowledge and exacting attention to detail have been an inspiration and kept my work on track from my first encounter with the data collection to the final draft of this paper. In addition, I sincerely thank ASTU, School of Electrical and Computer Engineering, Department of Electrical Power and Control Engineering for their support.

Table of Contents

List of Figures

List of Tables

List of Acronyms and Abbreviations

AC	alternate current
ASF	Average solar flux
AVS	Agrivoltaic systems
BIPV	Building integrated photovoltaics
Br	Ethiopian Birr
CAPEX	Capital Expenditure
DC	Direct current
DHI	Diffuse horizontal irradiance
DNI	Direct normal irradiance
GCR	Ground coverage ratio
GHI	Global horizontal irradiance
IEA	International Energy Agency
INRA	National Institute for Agricultural Research
IRR	Internal Rate of Return
LCOE	Levelized Cost of Electricity
MPPT	maximum power point tracking
NPV	Net Present Value
OPEX	Operational Expenditure
PV	Photovoltaic
PVWPS	Photovoltaic water pumping system
PVSyst	Photovoltaic system
SWERA	Sun and wind energy resource assessment

Abstract

This thesis illustrates a comprehensive study of using an agrivoltaic system in Aysit kebele, Afar Region, Ethiopia. This system is applied on an average wheat farm located in Aysit, which covers an area of 0.43ha. PV solar panels are implanted just above established farmland, with spaces beneath of PV solar panels in order to provide crops with the necessary solar radiation. Here, the profitability of a hypothetical Agrivoltaic system deployed on irrigated arable lands of northern Afar is analyzed. Solar panels plays a great contributions by providing shade in order to protect crop from the extreme heat conditions as well as providing energy to power farm systems such as pumping water for irrigation. The study provides detailed system sizing and dynamic modeling. System dynamic designing is done using MATLAB/Simulink which contains several models of subsystems such as PV arrays, DC-DC buck converter, DC-AC inverter, 3 phase AC motor, and centrifugal submersible pump. The dynamic modeling is developed based on the sizing of the system. This system can produce the required energy with relatively excellent controller dynamic performance, as per a MATLAB/Simulink simulation. To assess the system's economic viability HOMER software was used. The results were presented using a variety of economic measures, including internal rate of return (IRR), farm profit, levelized cost of energy (LCOE), and net present value (NPV). For the solar-powered irrigation system, all economic indications were positive.

Keywords : Agrivoltaic; Agriculture; Photovoltaic; Farming; Land Equivalent Ratio; Inverter*, Buck converter*;

Chapter One

Introduction

1.1 Background of the study

Ethiopia is located on the Horn of Africa, at latitude 3-15°N and longitude 33-48°E. Ethiopia has 1.13 million square kilometers in size. Ethiopia has a population of about 110 million people, making it the second most populous country in Africa after Nigeria, however 83% of them live in rural areas World population prospects. Despite the fact that Ethiopia has abundant natural resources and vast energy resources, the country is experiencing severe energy shortages in order to meet the country's expanding energy consumption, which is expected to increase by around 30% yearly (Dorling, 2021). Ethiopia's energy sector has the dual difficulty of limited access to modern renewable energy alternatives such as geothermal energy, solar energy, and wind energy. Although Ethiopia has achieved spectacular economic improvement in recent years, satisfying this development, the future will require dramatic increase of modern energy sources at a low cost.

The Afar region is one of nine governmental recognized regional states and is the homeland of the Afar people, with its capital city of Samara located at (11.45°N and 41°E) (Wolde-Ghiorgis, 2002). Its climate has bright average temperatures ranging from 27°C to 50°C. Currently the afar region's energy sector is reliant on hydropower energy for utility and basic life needs. Due to a variety of issues such as high capital investment, low load factor, insufficient voltage guidelines, and frequent power supply disruptions, the Afar region is experiencing significant energy shortages and so many non-electrified places. In Afar region rural communities, the cost of installing and maintaining hydropower energy lines is prohibitively expensive and inefficient. Furthermore, transmission losses will affect power supply consistency in rural grids (Bogale & Alemayehu, 2012; Hussein, 2016).

Solar radiation data on the earth's surface is important for a variety of applications in meteorology, agricultural sciences, engineering, and research. Ethiopia has an abundance of solar energy resources. According to a regional analysis of solar energy potential, the yearly average radiation ranges from low in western Ethiopia in the areas of (Gambella regional state) to high in northern Ethiopia around (Tigray regional state and Afar regional state) (Wolde-Ghiorgis, 2002). According to the sun and wind energy resource assessment (SWERA) studies, Ethiopia's solar energy resource wealthiest regions are primarily concentrated in Afar State in the northeast, the desert region in Somali State in the southeast, and certain western and southern regions. The Mid North region of Ethiopia has fewer solar energy resources. Tigray (246.48 W/m^2) has the highest average solar radiation power and annual total solar energy per unit area, followed by Amhara (240.34 W/m^2) and Afar (239.9 W/m^2).

Table 1.1. Solar Energy Resource in Different Regions of Ethiopia.

Region	**Area (1,000 km^2)**	**ASF (W/m^2)**	**T R P (TW)**
Afar	94.1	239.9	22.57
Amhara	155	240.34	37.26
Benishangul	49.5	232.52	11.5
Gambela	24.6	222.48	5.48
Oromia	320	223.96	71.66
SNNP	109.9	226.65	24.91
Somali	300.3	217.19	65.21
Tigray	50.2	246.48	12.38
Ethiopia	1,104	227.42	250.98

1.2 Statement of the Problem

Afar communities have been pastoralists for so many years. Since recent years their way of life begins being dependent on both pastoralism and agriculture because their cattle becomes extincted due to hard and warm temperature in the region. This region encompasses semi-arid and largely arid zones. The electric grid is inaccessible in most part of the region because 90% of the dwellers lives in countryside and the villages are loosely distributed. In order to achieve renewable energy target, space limitation must be minimized for future introduction of large scale solar plant. As a remedy to this land constraint, current agricultural regions can be utilised for PV solar generating, introducing new areas to the project. This is a hybrid system where crops and PV solar coexist in same land, which is known as agrivoltaic systems. Analysis for agrivoltaics should begin with the selection of acceptable crops, regions, and solar technology. A techno-economic analysis for agrivoltaic technology in Ethiopis was undertaken as part of this research, and it can be utilized as a pilot scheme for decision making when selecting agrivoltaic technology for appropriate crops and places. Moreover, in Afar region, the knowledge of AV system is not familiar and unluckily not introduced yet. This is why I am motivated and convinced to work on this project to solve my community main problem.

1.3 Research Questionnaires

- Why do not APV system being focus to be an economical solution for Afar Regional State?
- Afar Region is blessed with high intensity of solar irradiation as well as plenty of cultivable land; however, why it is not being effectively utilized?
- Can installation of photovoltaic panels using the space between crops AV system mitigate the trade-off between crop production and clean energy generation even when applied to crops that prefer moderate light in this region?

1.4 Objectives

1.4.1 General Objective

The main objective of this thesis is Design and Analysis of Stand-alone Photovoltaic Power System for Agriculture in Aysit Kebele Afar Region.

1.4.2 Specific Objectives

To achieve the main goals, this thesis work has the following specific objective

- To provide mutual benefits across the food–energy–water nexus in dryland using AV system, which uses the space between photovoltaic (PV) panels for crops.
- Component sizing and simulation using MATLAB software for solar PV water pumping systems.
- To establish a competitive and diversified agriculture because of the weight of this sector in the regional as well as national economy;
- To analyze optimal AP system by lowering the cost with the highest efficiency and reliability

1.5 Scope of the Study

The scope of this thesis work is tried to evaluate renewable energy issues and challenges in access to Agriculture in Afar region, North-East Ethiopia and to Design AV System using beneath PV panels for crops in Afar Region for the selected area based on their energy demand.

The scope of this research is limited to designing, analysis and Simulation of each PV system components and modeling is conducted by using MATLAB software/Simulink.

There are some restrictions to the study as well.

It was based on theoretical assumptions, with no practical AV system installed at the designated location.

Even though Solar system is designed for 80ha, the AV system is designed for only 0.43ha

Multiple assumptions are made for the input parameters in economic and farming calculations, both on the cost and income sides.

1.6 Significance of the Study

The benefits of combining PV and agriculture will be significant for a variety of ecosystem services, including:

(1) Water: maximizing the efficiency of water used for plant irrigation by decreasing evaporation from soil and transpiration from crop canopies,

(2) Food: avoiding photosynthetic depression as a result of heat and light stress, allowing for more carbon uptake for growth and reproduction and

(3) Energy: transpirational cooling from the crops side lowering temperatures on the underside of the panels, which could improve PV efficiency. And an additional benefit is It will motivate the researchers to be familiar with the solar technologies and make initiation to do another research problem on another case study area and develop his/her knowledge. It will benefit the government:-that is, it supports the government by decreasing the budget that is allocated to the irrigation to the societies with low cost.

1.7 Organization of the thesis

Chapter 1 of the thesis discussed the introduction, background, problem statements, Research Questionnaires, objectives, the significance of the study, the scope of the study, motivations of the research, limitations of the research.

Chapter 2 of the thesis discussed the theoretical background, Potential of Agrivoltaic system, and is written in a format of a literature survey of the agrivoltaic systems, PV water pumping system It includes the steps of selecting a proper solar water pumping system as well as the main principles of the operation of solar pumps.

Chapter 3 of the thesis discussed an outline of the AV system sizing in a form of a case study, which will define the sizing of the pumps and the photovoltaic, converter, and batteries sizing using Homer and PVsyst software. Also, the possible energy storage methods are provided.

In Chapter 4 the results of the research are demonstrated and further discussed, which includes sizing and modeling simulations outcomes as well as water and system cost.

In addition, Chapter 5 discussed the conclusions regarding the completed work as well as the list of resulting publications. Recommendations on this subject are provided as well. The appendices are added at the end of the thesis.

Chapter Two

Literature Review

2.1 Theoretical Background

To date, three types of agrivoltaic systems, which enable crop and electricity production on farmland simultaneously, have been proposed (Figure 2.1). The first type, which used the space between PV rows for crops, was proposed in the early 1980s (Adolf Goetzberger & Zastrow, 1982) . Solar plants using ground-based PV panels compete with agriculture for land. Solar panels and crops compete for solar radiation. This type of AV is still in practice in some countries. The second type consists of stilt-mounted PV modules above the crops. The third type is a PV greenhouse, in which part of its transparent covering is replaced by PV modules. Because it allows continuous food production and electricity generation throughout the year, the use of PV for greenhouses is a promising solution for the competition for land resources between food and energy production.

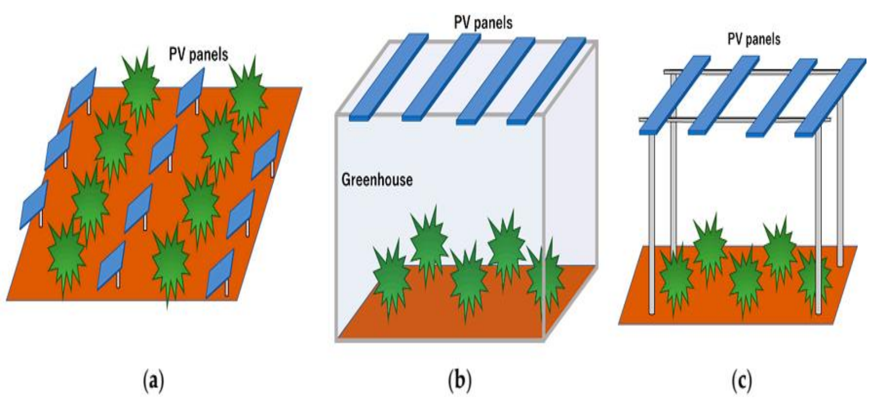

Figure 2.1: Three different types of AV system: (a) ground mounted photovoltaic (PV) panels, (b) a PV greenhouse, and (c) a stilt-mounted system.

All the three types of AV have their own pros and cons. There are implications when the modules are installed high on the ground. Taller configurations, for example, may cause several public concerns or even rejection due to the negative impact (visibility is recognized as one of the complex objective factors that contribute to the visual impact of PV) (Dinesh & Pearce, 2016). The use of higher mounting structures have not only an impact on social acceptance, but would also have a significant impact on installation costs and environmental impact. In the German context, the additional cost associated with elevating the PV modules (mounting, installation, and site preparation costs) is estimated to be more than double (increasing from 0.3 EUR/kWp to 0.7 EUR/kWp when compared to ground-mounted PV (Marrou, Dufour, & Wery, 2013).

Studying the optimization of all the parameters for the AV system is the first aim of this master thesis. The optimal parameters to design both the PV plant and the agricultural production are defined thanks to literature.

In literature, there are many studies about AV. Ground mounted (tilting the solar panels at some specific height) AV method is particularly effective for growing lettuce, pepper, tomato, aloe vera, maize, and pasture grasses (Adeh, Good, Calaf, & Higgins, 2019) . In one of the studies, it is mentioned that the product efficiency has increased by 60%–70% by this method (Dupraz et al., 2011).

Existing studies have focused on AV with stilted solar arrays. Farm experiments with stilt-mounted PV modules were recently reported in France (A Goetzberger & Zastrow, 2015) and the United States (Majumdar & Pasqualetti, 2018).

They indicated that the system of planting shade-tolerant crops does not decrease land productivity. Adoption of AV systems may therefore require minimal adaptation of cropping practices. The first reported AV farm experiment was performed in Montpellier, France in 2013 (A Goetzberger & Zastrow, 2015). They grew lettuce crops with a system consisting of 0.8-m-wide stilt-mounted PV modules, mounted at a height of 4 m and tilted at an angle of 25°. The same area of land was used to successfully produce both electricity and food. Their results showed that shading created by the PV arrays had no significant effect on the lettuce yield. The growth rate below the PV panels was not reduced except during the juvenile phase of the crop.

In recent years, AV systems have been the subject of numerous studies due to their potential in the food–energy nexus. Demonstrative projects with new conceptual designs based on PV modules for covering open fields have shown promising results through optimizing light availability while reducing the need for irrigation and protecting from extreme weather phenomena.

A small-scale research plant was installed in Arizona at the Biosphere 2 Lab in August 2016. The research group focuses on common agricultural species for drylands such as peppers, jalapeños and cherry tomatoes (Weselek, 2019). The AV system is 3.3 m off the ground with a tilt of 32° and 1 m of spacing between each row of PV modules.

Research in the field continues to progress at a furious pace. Aside from these pilot projects, AV have triggered much interest in the research community that explores the potential from different disciplinary perspectives. Practical issues, such as the solar power potential by land cover type (Adeh et al., 2019) the water use efficiency in drylands (Elamri, Cheviron, Lopez, Dejean, & Belaud, 2018) or groundwater stressed regions. The implementation in peri-urban agriculture areas (Majumdar & Pasqualetti, 2018) or the viability over shade-intolerant crops in specific geographical locations (Malu, Sharma, & Pearce, 2017) and (Sekiyama & Nagashima, 2019).

Although research in the field continues to progress, excitement around AV remains high enough that commercialization is well underway. Globally, the installed capacity of the AV continues to climb. It is estimated that 2200 systems have been installed worldwide since 2014 (Japan is probably the country where the most AV farms were installed, with over 1992 AV farms which produced about 0.8% of total PV energy in 2019), leading to a capacity of about 2.8 GWp as of January 2020 (Schindele et al., 2020). In 2018, the first AV field was built in the east Pyrenean region (France). This field has a capacity of 2.2 MWp installed on 4.5 ha of vineyards. Today, the company focuses on the development of large-scale demonstrator systems of dynamic AV technology in orchards, grapes and market gardening. Some examples of the main issues related to the use of co-located PV on cropland and the solutions commonly proposed to solve them are shown in Table 1.

In parallel to the development of the new field-tested designs, the continuously scientific progress in PV has extended the range of design solutions by using different technologies which optimize the light absorption of the modules in different regions of the light spectrum, so that the light resource can be shared for both purposes: energy generation and crop growth. As can be seen, AV does not follow classical PV system design practices where parameters such as tilt and orientation angles are optimized to maximize electricity production choosing slopes close to the latitude and orientations facing the equator. Moving PV to include farm activities is an ongoing challenge since energy performance sometimes conflicts with optimal agricultural development and landscape preservation issues, and thus involves multiple design adaptations according to the local climate conditions, crop type, energy needs and landform (Simonneau et al., 2017). A new list of requirements must be addressed to ensure and understand the tight connection between energy, food production and space. This paper therefore aims to analyze the different design possibilities that focus on the energy performance of the PV system, extending to agriculture objectives and presenting an original contribution in the cognitive trans-disciplinary approach for describing and classifying the AV system, which harmonizes different disciplinary issues in a unique vision, making room to consider landscape issues.

Table 2.1: Barriers and solutions to implementation of AV in open-field systems (Sekiyama & Nagashima, 2019).

Topic	**Design Related Solution**	**Technology Related Solution**
Minimizing shadows on crops (biomass yield)	Optimal design: Distance between the arrays of modules (the stripes)Distance of the modules from the ground	Sun-tracking systems Semi-transparent PV modules (by spacing PV cells) Light-selective PV devices
Maximizing electric energy generation	Optimal planning: Avoiding sharing losses from surrounding elements (structures, buildings, trees, inter-row shading of the PV modules should be minimized)	Highly efficient systems (e.g., sun-tracking systems) Highly efficiency modules or technologies (e.g., bifacial module technology)
	Optimal design: Azimuth facing equator and tilt close to latitude	
Social acceptance (landscape dimension)	Optimal landscape design: Pattern of PV arrays aligned to the parcel, Natural fences and low height structures to minimize visual disturbance, Use of marginal areas Removable systems	New materials for structure
	Optimal design: Different tilt, azimuth and height to reproduces the orography of the land	
	New business models: Higher economic efficiency per land unit (farmer perspective) Benefits for local economy and employment (tourism, local recreation, etc.)	

2.2 Potential of Agrivoltaic system

An AV approach was developed for the first time in 1982 (Adolf Goetzberger & Zastrow, 1982). Although it received little attention at initially, this issue grew in prominence over time. The main purpose of the AV system is to grow plants while generating electricity on the same land. AV system provide mutual benefits from between the food–energy–water consumption in drylands (Barron-Gafford, 2016). The AV system will inevitably cause changes in microclimatic conditions under the panel. The water consumption balance will shift as a result of the decrease in solar radiation under the PV panel, and water savings will be achieved (Weselek, 2019). Furthermore, this technology not only expands agricultural grounds and saves water, but it also boosts crop output.

Sensors can be installed in the underground parts of the steel structures that maintain the photovoltaics in the air to improve crop efficiency. As a result, information in terms of vitamins and minerals required by the product can be retrieved (Jia, Li, Dong, & Zhang, 2011). This strategy is very effective for growing lettuce, pepper, tomato, aloe vera, maize, wheat, and grazing grasses (Ravi et al., 2016; Weselek et al., 2019). According to one of the research, this strategy boosted product efficiency by 60%–70% (Dupraz et al., 2011).

Fig. 2.2 shows a diagram of an AV system. "b" represents the distance [m] between PV module rows used in agriculture, "a" represents the horizontal projection of the PV [m], "t" represents the tilt angle in degrees, and "h" represents the height [m] of the steel structures.

Standard farming equipment must be allowed to move between rows to harvest the produce without damaging the PV modules, so the height of the steel constructions and the spacing between PV rows must be adequate (Coşgun, 2021).

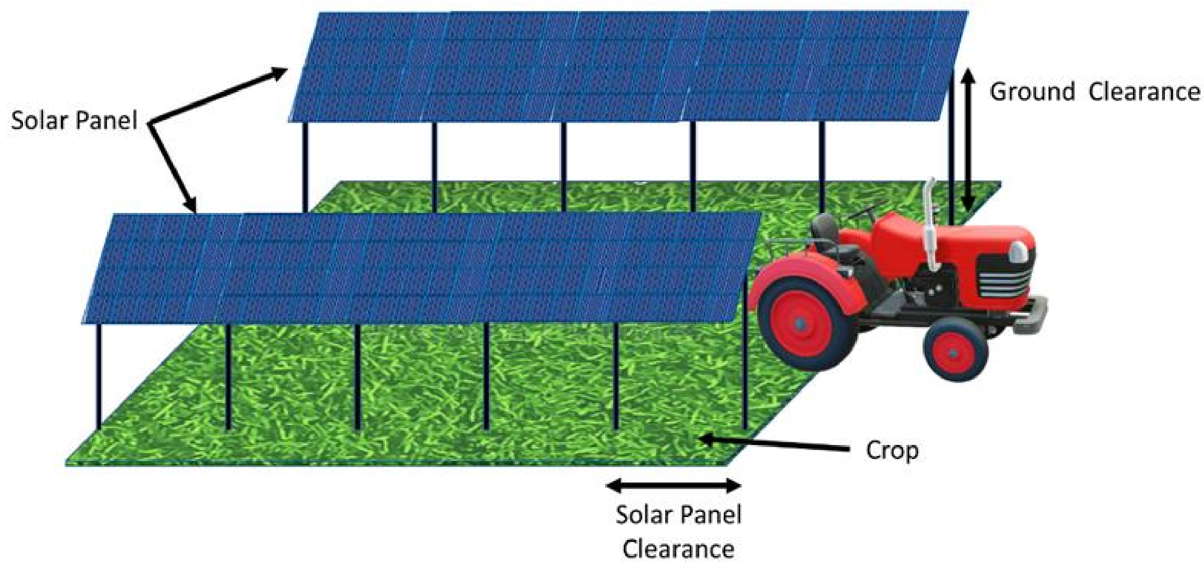

Figure 2.2 Solar agriculture farm where solar panels are co-located with crop

In standard PV plants, there is usually 6–12 m of space between two rows of PV arrays. The purpose of this area is to keep the PV from casting shadows on the next row, and it must be suitable for harvesting the crop. The following factors are critical for plant growth in each row of a solar PV system.

The plant's height, diameter, and number are all important factors to consider. In cereals, irradiance is particularly important for growing grains (Artru et al., 2017; Jia et al., 2011; Li et al., 2012). Although other plants, such as carrot, radish, leek, beet, lettuce, sprouts, cauliflower, spinach, broccoli, pepper, tomato, aloe vera, maize, and pasture grasses, do not require much sunlight to grow. These crops are shade-loving agricultural produce that can grow under a stilt-mounted AV system.

A preliminary study by Fraunhofer ISE at a site in India's federal state of Maharashtra indicates that the effects of shading and reduced evaporation from AV systems can boost tomato and cotton yields by up to 40 percent (Trommsdorff, 2019). The researchers got the land use efficiency for this region to nearly double as expected.

In the course of a project under the EU's Horizon 2020 program, in cooperation with partners in Algeria, Fraunhofer ISE researchers investigated the impact of AV on the water supply. Aside from reduced evaporation and lower air and soil temperatures, rainwater collection with PV modules also plays a role. Rainwater collection using the modules is of great interest for many countries, including parts of Germany, especially as the frequency of droughts increases.

2.2.1 Design criteria of AV System

Solar panel erecting characteristics in AV systems differ differently from those in a traditional solar power plant.

In addition to food production, the installation of such systems in farmers' fields may generate additional cash from the sale of power.

In a 1 ha cropped field, 240 to 480 kW capacity systems might be installed, according to estimates. PV arrays of one-row PV modules with 3 m interspaces between arrays, PV arrays of two row PV modules with 6 m interspaces between arrays, and PV arrays of three-row PV modules with 9 m interspaces between arrays have all been installed at CAZRI in Jodhpur with a total capacity of 105 kW. Solar PV modules were mounted perpendicularly on a permanent MS iron angle framework.

The PV system is considered in its multifaceted features, and it is described accordingly in terms of spatial features, energy features and engineering features. In this regard, Oudes and Stremke (Oudes & Stremke, 2021) have recently published a comparative study that analyzes solar landscapes by examining spatial properties, visibility, multi-functionality and temporality, showing the imperative need to build analytical frameworks for analyzing PV systems in a holistic manner, evaluating both individual properties and the system as a whole.

The spatial features are broken down into pattern and patch.

The pattern description gives an account of the spatial arrangement of the PV modules through the size (qualitatively: with large patches, with small patches; quantitatively: width, length, area); geometry (parallel stripes, checkboard, islands); type (continuous, dispersed, random); and density (porous, dense, LAOR). (In assessing as “porous” or “dense” a certain AV pattern, here it is considered that about 40% of PV area/land area is usually standard for AV systems.

The energy features are broken down into nominal power, number of modules, density of power, land use energy intensity, normalized yearly energy generation and PV module technology. For each of these categories, appropriate metrics are considered. The engineering features are broken down into system typology (fixed, sun-tracking one axis/two axis), modules supporting system (material, technology, weight) and foundations (material, technology, weight).

The “pore space” (what is in between the PV modules, and the ground) in the AV pattern is described in terms of three-dimensional pattern features, crop features (type, homogeneity, plant’s height and seasonality) and energy features.

The three-dimensional pattern is an original descriptive expedient that the authors propose for characterizing an AV system from the performance point of view, based on the three-dimensional features of its pattern, referring to a unitary land area.

The features of the three-dimensional pattern are average volume, area, zone type (irradiation and connectivity) and crop density (crop area/total area %). The average volume considers the pore space area (total land area minus the area corresponding to the projection of the PV modules on the ground) multiplied by the height of the modules from the ground (considering the lowest line of the modules) (see Figure 2.3).

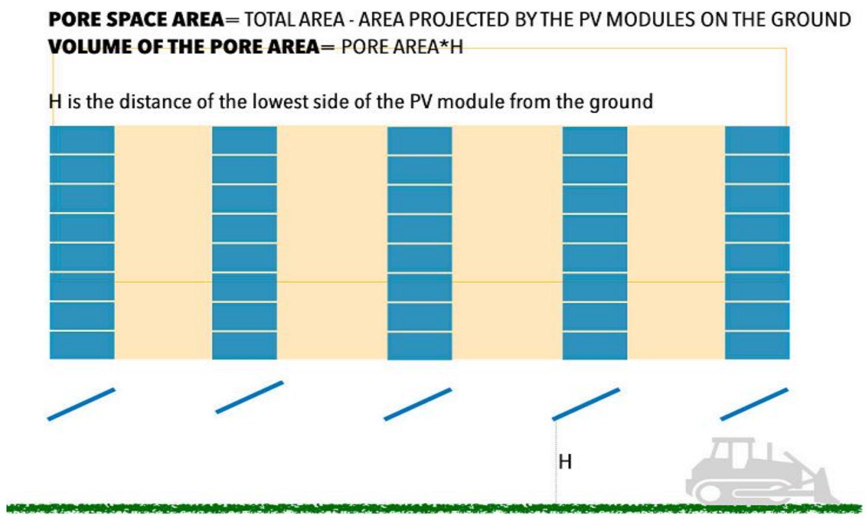

Figure 2.3. The three-dimensional pattern of the AVS

The zone type qualitatively describes irradiation and connectivity that characterize the pore area. Connectivity is defined as the degree to which the landscape facilitates or impedes movement among resource patches. There are zones with high, medium and low irradiation, and to these correspond high, medium and low connectivity.

Irradiation and connectivity basically depend on the degree of porosity of the PV pattern and on the height of the PV modules from the ground: the more porous the pattern, the higher the irradiance (and therefore the irradiation), whereas a high distance from the ground implies generally a higher connectivity and a lower irradiance.

Figure 2.4 shows the influence of module height on irradiance. Given a certain PV pattern and sun altitude, in fact, depending on the height of the modules from the ground, it is possible to see that the dynamically shaded area decreases with the increase in the height for the same area under the PV arrays. In Figure 2.4a, the color ranging from blue to orange provides a qualitative assessment of the height effect on the irradiance, and therefore on the irradiation. A quantitative assessment is more complex (a simple analysis is shown in Figure 2.4b) and requires a simulation effort, as the degree of irradiation depends on the dynamic shading on the ground. Regarding the connectivity, Figure 2.5 shows that, given a certain PV pattern, the connectivity increases along with the increase in the height of the modules from the ground.

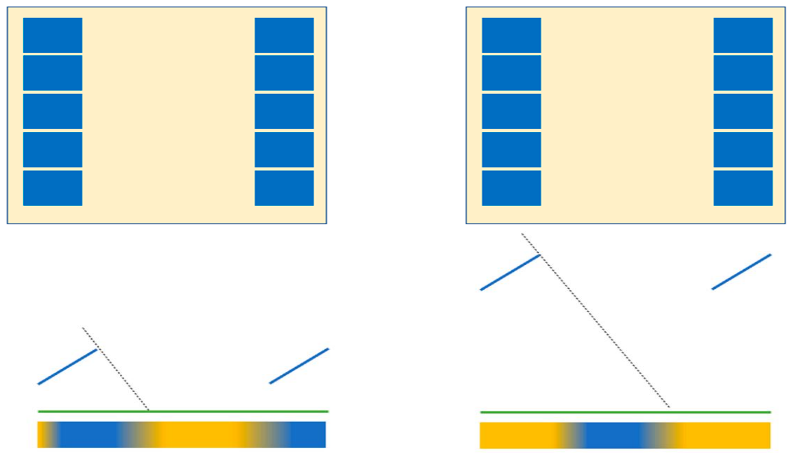

(a) Qualitative assessment. Shaded area decreases with the increase in the height for the same area (crop area) under the PV system.

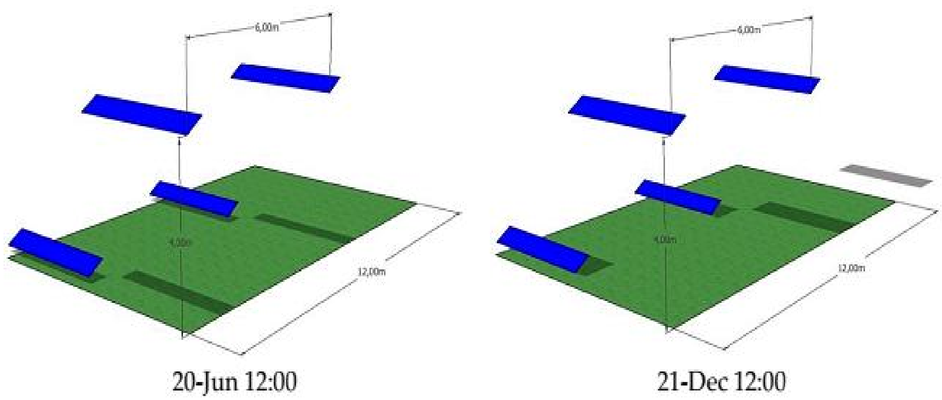

(b) Simulation for two cases: solar arrays elevated 0.5 m and 4 m above the ground. When raising the structure, the shadow pattern falls on adjacent areas and does not affect the area beneath the PV modules where the agricultural activity is hosted.

Figure 2.4. Irradiation vs. Height of the photovoltaic modules on the ground.

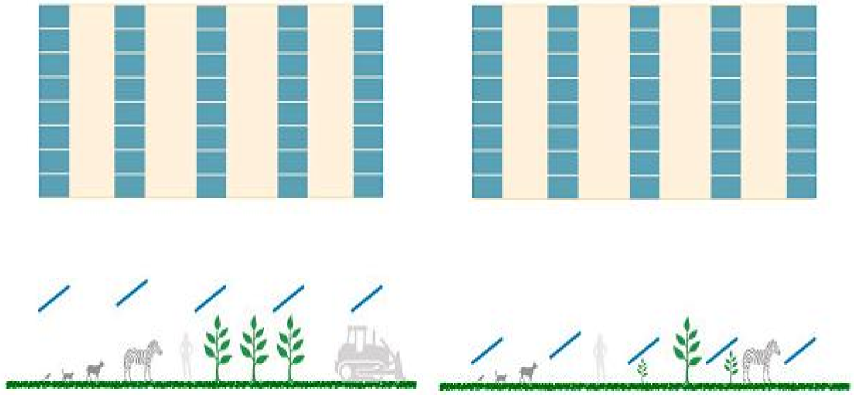

Figure 2.5. Photovoltaic pattern and connectivity

Based on these considerations, zone types have been defined as high irradiation and high/medium/low connectivity, medium irradiation and high/medium/low connectivity and low irradiation and high/medium/low connectivity.

Then, the crop density is considered as the ratio between the crop area and the pore area (%). The crop features are plant's height (uniform; non-uniform, and is uniform: height; if non-uniform maximum, minimum and average height); seasonality (12, 6 or 3 months).

2.3 Crop management

The selection of crops suitable with the installation of PV panels using the space between crops is a key aspect for the success of the project. Indeed, it will modify its sun exposure, the shade, the water availability etc. A study based on literature review will be performed to highlight the parameters of the crop affected by the PV plant and to determine which crops are the best suitable for APV system.

2.3.1 Key parameters for crop selection

• Shade Tolerance

The main consequence of the installation of a PV plant above crops is the creation of shade (Adolf Goetzberger & Zastrow, 1982). It is important to know precisely the shade tolerance of crops under the panels that is to say their ability to tolerate low light levels.

The implementation of AV systems involves changes in cropping practices. Plants able to maximize their radiation use efficiency should be prioritized. Light reduction has not necessarily a harmful effect on crops that can adapt and improve radiation interception efficiency. The lack of studies on the large majority of plant precludes any conclusion on the impact of shade on plant growth (Proctor, Murthy, & Higgins, 2020).

• Water stress and irrigation

Shade provided by PV panels could prevent the damaging effect of excessive light and it could limit evapotranspiration during peaks of evaporable demand. The plants that will benefit most from the system will be plants with high water requirements and plants that are not resistant to water stress (Dupraz et al., 2011).

• Height

Crops under the panel should not exceed a certain height during their lifetime. Panels are elevated at 3 or 4 meters (Sekiyama & Nagashima, 2019). In the western Great Plains, where drought occurs frequently, tall wheat cultivars are preferred over semi-dwarf wheats because they emerge better in dry soils and leave more residue (Burleigh, Allan, & Vogel, 1965) which improves soil structure and helps control erosion (Skidmore & Siddoway, 1978). Conversely, semi-dwarf wheats are desirable in the eastern Great Plains where rainfall is higher. They are resistant to lodging, have high yields, and a good response to fertilizer (Pearman, Thomas, & Thorne, 1978). when water is not limiting.

• Crop rotation

It refers to recurrent succession of crops on the same piece of land either in a year or over a longer period of time. The objective is to get maximum profit and ensure the preservation of the fertility of the soil and to keep a uniform distribution of soil nutrients (Mavani, Chauhan, & Joshi, 2019). Crops are divided into exhaustive crops and less exhaustive crops. It is important to take into consideration crop rotation before the installation of the AV system to ensure the sustainability of the agriculture under the panels. Every crop decided before the construction of the PV plant should respect criteria mentioned here.

The AV system increases the shade for crops and it is a protection against climate change consequences. It is interesting to target crops which are badly affected by climate change and for which AV systems will contribute to improve their yield. Crops that can be successfully grown in interspaces of the established AVS at Aysit include wheat (*Triticum aestivum),* mungbean (*Vigna radiata*), moth bean (*Vigna aconitifolia*) and clusterbean (*Cyamopsis tetragonoloba*) can be grown under irrigated situations. For cultivation in below panel areas, few vegetable crops e.g. cabbage (*Brassica oleracea* var. *capitata*), onion (*Allium cepa*), chilli (*Capsicum annum*) and garlic (*Allium sativum*) may be selected. These crops are expected to modify the micro-climates below PV-module in reducing the temperature and thus PV-based electricity generation will be optimum. Moreover, the crop coverage in between PV arrays will also check the erosion of soil and thus will reduce the dust load on PV module.

In the last decades, efforts are being made in Ethiopia as well as throughout the world to supply water to meet drinking and irrigation needs in remote regions. Thus , for rural applications , various established models (Arab, Chenlo, & Benghanem, 2004), sizing techniques of photovoltaic water pumping system (PWPS) have been reported in the literature.

2.4 Crop Water Requirements

The table below depicts the impact of climatic conditions on crop water needs. When the crop is cultivated in hot temperatures, low humidity, high wind speed, and sunny conditions, the crop need more water than when the constraints are somewhat.

Table 2.2: Effects of Climatic Conditions on Crop Water Needs (FAO)

Climatic Factor	Crop water need	
	High	Low
Temperature	hot	cool
Humidity	low (dry)	high (humid)
Windspeed	windy	little wind
Sunshine	sunny (no clouds)	cloudy (no sun)

2.5 PV water pumping system

PV systems are classified based on their component style into either stand-alone or grid-connected systems. Grid-connected systems generate and inject electricity directly into the utility grid. An individual could install PV array on the house roof, and also it could be used in large-scale PV plants. A converter is employed to convert the PV array's generated DC power to AC with the same grid specifications. The inverter is programmed to protect the system in case it stops converting and supplies power when the grid is off. PV grid-connected systems have become attractive for both governments and industry. Furthermore, they have started to become attractive for individuals, especially in countries with high electricity costs. Stand-alone PV systems operate separately from the grid to provide proper AC or DC loads. The PV arrays are mainly used in rural and isolated areas, far away from the grid. Stand-alone PV systems have many forms. These include a PV array only, or one connected to another renewable or non-renewable source widely known as a hybrid system.

Some of these systems are renewable using geothermal, wind, hydro, and solar thermal energy sources. Others use non-renewable sources like diesel or natural gas generators. A simple stand-alone PV system contains PV modules, a charge controller, and batteries (optional) for storage. They also contain an inverter if an AC load is needed. As the use of batteries adds costs and maintenance, it is easier to use the PV module directly to generate the required load power in the daytime. Many applications like water pumping systems operate during daytime only (Fudholi et al., 2014).

According to (Arrouf & Ghabrour, 2007), the technology of solar cell is growing fast.(Alkarrami, Iqbal, Pope, & Rideout, 2020) stated that solar photovoltaic water pumping systems are the most widely used renewable energy source water pumping system for irrigation and domestic use. (Abu-Aligah, 2011) also stated some advantages of solar PV system: unattended operation, low maintenance, easy installation, and long life. In this situation the Government of Afar region is promoting alternative sources of energy to meet the energy deficiency. Many governmental and nongovernmental organizations are encouraging people to go with renewable sources of energy. Afar Regional State Government is giving subsidies for alternative energy projects. Yet, there is no solar irrigation pumping system exists in Afar region. (Glasnovic & Margeta, 2007) developed a mathematical model to acquire an optimal PV system by considering not only water demand or irradiance but also including natural process, that is, climate, hydrology, boreholes, pumping system, irrigation, agriculture, and power supply. (Arrouf & Ghabrour, 2007) modeled and simulated a pumping system fed by a PV generator in MATLAB/Simulink. The system included PV generator, DC-AC converter, asynchronous machine, and centrifugal pump. They simulated each part of the system separately under specific condition and the result satisfied their expected values. (Bhende, Mishra, & Malla, 2011) designed a stand-alone PV water pumping system without battery storage in MATLAB/Simulink. The system consists of Perturb and Observe (P&O) algorithm based MPPT (Maximum Power Point Tracker) for improving efficiency. He described the control strategy to regulate the water discharge for a single induction motor as well as multi-induction motor. (Harishankar, Kumar, Sudharsan, Vignesh, & Viveknath, 2014) proposed a controlled irrigation system in which the outlet valve of the tank was automatically regulated using controller and moisture sensor to control the flow rate of the water from the tank to the irrigation field to optimize the use of water. (Pande, Singh, Ansari, Vyas, & Dave, 2003) proposed a PV water pumping model to ensure uniform irrigation in arid regions using Openable Low Pressure Compensating (OLPC) drippers and manual tracking.

According to (Anis & Nour, 1994) increasing the water tank size is more economical than increasing both array and battery size. Finally, concluded that for consecutive three seasons' irrigations, the unit cost of water is cheaper in case of PV water pumping system comparing with diesel engine system. (Abu-Aligah, 2011) did the cost and reliability analysis between PVDC and diesel engine system and PVDC system turned out as more reliable system. He also did the Life Cycle Cost (LCC) analysis for a period of twenty years and found that the solar energy system was cheaper although the initial cost was high for it. (Senol, 2012) performed economic analysis for three different cases: (i) no subsidy, (ii) 50% subsidy (not including PV module cost), and (iii) 50% subsidy (including PV module cost). The investigation proved that PV powered pump is preferable.

PV water pumping, in general, is cost-effective in a rural area, so it is a good option for isolated desert areas. The PV system operation reduces environmental pollution in addition to operating the water pumping system. Portable drinking water and irrigation water are essential in rural areas. Solar PV systems have become attractive to supply power for water pumping systems due to the improvements made in PV efficiency and the reductions in PV prices. PV water pumping systems are used for irrigation, watering of livestock, and village water supply.

Photovoltaic pumping system description

Water pumping for irrigation for rural communities represents an important area of stand-alone PV systems; these systems usually consist of a photovoltaic generator, source of water, a water storage tank, batteries and an AC pump (see Fig.2.6).

The role of batteries can be played by the water storage tank and the electric power load demand L in now replaced by water demand. If expressed in Wh/day, this represents the energy needed to pump the required volume of water demanded by the user into the storage tank. These considerations show that PV pumping systems can be sized in a similar way than PV systems with other applications.

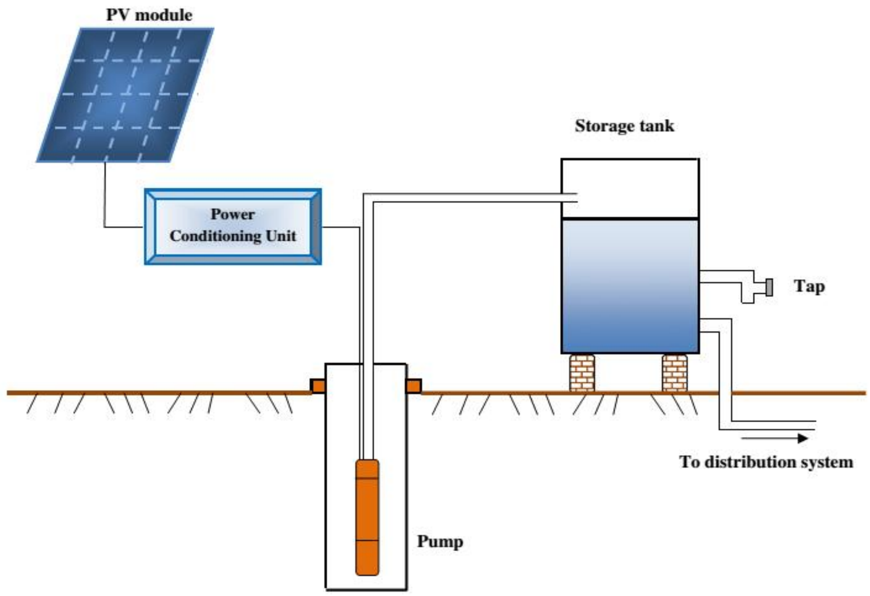

Fig. 2.6. Block diagram of a stand-alone PV water pumping system.

2.6 PVSyst Software Simulator

There are numerous software programs available to calculate the annual PV solar generation of a particular location, which is a difficult process. Among them are HOMER, RETScreen, and PVSyst. Continuous variations in environmental parameters such as sun irradiance, incidence angle, panel temperatures, inverter losses, and other Miscellaneous losses will be simulated by these softwares. Further sun tracking systems and specific technical data from panel manufacturers will be carefully considered for the calculations. The selected location's accurate solar radiation and temperature database will be provided. PVSyst is a simulation software that is utilized in this research to anticipate prospective annual generation based on a specific location utilizing its inbuilt databases.

CHAPTER THREE

MATERIALS AND METHODS

For my methodology, I concentrated on the engineering and business aspects of this thesis. The engineering portion concerned how I envision the Agri-PV system work, look for existing instances in other parts of the world and design and plan for the solar system's installation. The business side includes the project's profitability and what is obtained in terms of income and cost savings, among other things. The approach used to reach the overall goal of the study includes: a literature review of various journal publications, articles, and conference papers on AV systems.

3.1 Data Collection

Data was gathered through a combination of literature review and a field survey using a series of standardized questionnaires. Survey questionnaire was designed for the owner of the farm (Afar Region Agriculture Bureau). A reference farming village Aysit was selected in the Afar Region, Ethiopia. Local common crop types, cropping seasons, land preparation practices, reference harvest quantity in reference farm size, agro-processing activities, post-harvest management, local market for the products (or self-consumption), market price both for selling and purchasing agricultural-products, costs for farming activities, and so on are all included in the data on the farming side. The cost of the solar plant (capital cost for installation, operation), power generation, and selling prices are all data points on the solar PV side (surplus selling and self-consumption). Solar radiation, precipitation, temperature, and other climate data were obtained from a meteorological/satellite database (Meteonorm V.8).

System for Irrigation, specification of water access projects which has done previously and some other related sources, which includes, theoretical knowledge of solar energy technology, for solar PV water pumps available in the literature. The data used as an input for each of the analysis is collected through PVGIS, IEA, EEPCo and previously conducted studies, journals and reports, including web sites and internet links for there is hardly any updated and accessible data for the country, such as National Meteorology Agency (Samara Agricultural and Research Institute Office) and NASA.

3.1.1 Data Analysis

Once the investigation of data would complete, expected to collect from the field and the data obtained from secondary sources and cross-checked, verified, analyzed and interpreted data theory on basis of the problem and generalizing principles using appropriate theories and the sizing the system will be carried out by using some useful tools such as Homer and PVsyst software.

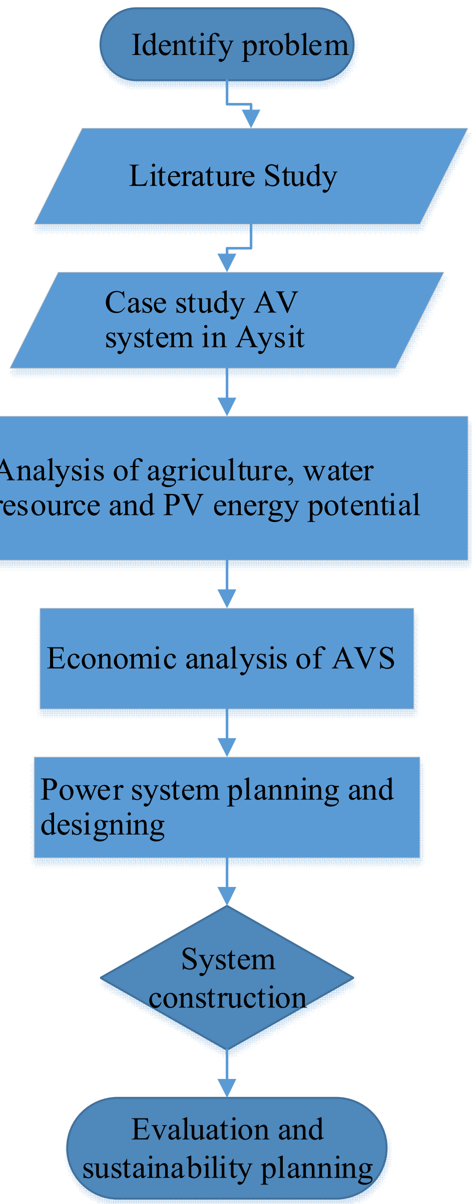

Figure 3.1: Flowchart for the proposed system

3.2 Site analysis

This study is applied on an average farm which is located in the northern area of Afar region, Dalol woreda having a coordinate of 14.23N, 43.12E. The farm mainly consist of 80 hectares of Wheat cash crop. It's surrounded by desert where there is no grid connection. Its location considered as a remote area due to the hardships in diesel transportation. The case study is 936 km far away from the capital Addis Ababa and 356 km from the region capital Semera.

Instead of making traditional solar PV farm, from 80 ha it is decided that to undergo AV system on 0.43 ha of the arable land and only AV system with its pumping system considered.

The climate in Aysit is hot desert, which experiences a mean annual temperature of 30 °C and is characterized as having most precipitation with a summer rains. Average precipitation is limited to <22 cm. Summers are hot, with air temperature regularly averaging 40.49 °C and soil surface temperatures exceeding 45 °C. Winter temperatures are relatively colder. Summer season agriculture in this region is primarily a mix of vegetables, with wheat, onion, tomato and maize being most prominent.

The field survey confirmed that the case study village of Aysit has significant problems with water and energy supply. This has a direct impact also on agriculture and livestock production. Thus, one of the important issues, the irrigation water supply, have been analyzed to compare the farm production without and with irrigation systems. Two irrigation techniques-diesel and solar energy driven pumps have been considered for comparison.

The site involves replicated rows of wheat crop species growing in under a raised solar PV panel array (AV system). Each of these areas is approximately 1956*992*34 m. The fixed panels within the AV system are 2 m above the soil surface at their lowest point. All panels face south, at a latitude angle of 14.21N. There is 3 m of spacing between each row of PV panels.

An irrigation system was established that delivered equal amounts—in terms of rate and cumulative application—across the control and AV plots. Equality in irrigation delivery was confirmed on measuring total volumes at random emitters across the plots. We planted replicate plants of wheat crop agricultural species that represent different adaptive niches for dryland environments. Seeds were planted within a matrix of the same 'Garden Blend' in December 2021 in under PV panels.

The irrigation system was a typical pressurized system. We performed calibrations on the irrigation system's delivery consistency once I a season. We used graduated cylinders to determine rates in terms of volumes per minute to ensure that the irrigation emitters were providing comparable amounts of water despite varying distances from the irrigation control box. We kept these measurement stations up for a complete growth season to record variance due to solar angle and extremes associated with hot and cold periods near the end of the season.

3.2.1 Meteorological data

The weather data used is taken from Meteonorm (2021) for Dallol. Monthly values of global and diffuse radiation are presented in Table 2.1. For calculating the maximum voltage in the circuit it is necessary to know minimal possible daytime temperature for the place. It is assumed to be 30°C.

Table 3.1 Monthly Meteo values for Dallol, Ethiopia (Meteonorm, 2021).

	Global horizontal irradiation kWh/m²/day	Horizontal diffuse irradiation kWh/m²/day	Temperature °C	Wind Velocity m/s	Relative humidity %
January	5.11	1.90	28.3	3.29	61.4
February	6.28	1.96	30.3	3.73	43.6
March	6.71	2.08	32.4	3.24	48.5
April	7.54	2.05	34.6	3.19	40.5
May	7.31	2.29	36.0	3.35	38.6
June	7.35	2.51	36.5	3.47	31.5
July	6.62	2.74	37.3	3.15	35.0
August	6.42	2.57	37.3	3.21	38.8
September	6.74	2.39	35.6	3.41	43.1
October	6.90	1.75	33.8	2.53	37.3
November	5.86	1.71	32.3	3.55	44.9
December	5.88	1.47	28.9	3.48	41.8
Year	**6.56**	**2.12**	**33.6**	**3.3**	**42.1**

3.2.2 Proposed AV System

The field study was performed on a 0.4 ha solar array located on the Aysit kebele wheat Farm. The PVPs have been arranged in south orientated strips, 2 m wide and inclined southward with a tilt angle of 14°. PVPs have been held at 1.2 m above ground at lowest point and 2 m above the ground at the highest point. The distance between panels is 3 m as shown in Figure 3.2. The solar array system has a total capacity of 92 kilowatts. The selected crop is tropical wheat with 0.8m above ground. As shown in Figure 3.2, the data were collected from localized zones including areas below solar panels and a control area outside the AV system. The site soil is Chehalis silty clay loam with a top soil pH of 6.23 and 6.06% organic matter content.

PV-modules are installed in AV system at an inclination angle equal to the latitude of the place of installation. Thus, shade of PV-module is generated at leeward side on ground surface as per the movement of sun. To avoid the shade of one PV array on the next array, a separation distance between two arrays is maintained. Moreover, area below the PV module are utilized to grow crops since PV modules are fixed over mounting structure at a certain height from ground surface. However, growing crops under shade requires selection of suitable crops which have certain degree of shade tolerance. The shaded portion at interspaced area varies from morning to evening as per zenith angle and azimuth angle of sun's position. However, the shade is dynamic following the sun's movement and thus the shaded portion on ground surface does not remain static but changes with time in a day. Available photosynthetically active radiation (PAR) on shaded ground surface was also found significantly lower (84.5 to 127 mmol cm^{-2} s^{-1}) than open sun condition (243-1296 mmol cm^{-2} s^{-1}).

Height of crops is a key parameter for selection of crops for AV system because tall-growing crops may create shade on PV-module and thus reduce the PV-based electricity generation.. Therefore, in our case, the selected wheat crop height is 1.2m above ground crops with low height (preferably shorter than 1.5 cm) and which tolerates certain degree of shade and require less amount of water are most suitable for AVS. Crops can be cultivated in AVS at interspaced areas between PV arrays and at areas below the PV arrays. Area available for cropping purpose changes as per design of the installation. The interspace and below PV module areas available for cultivation of crops in a typical AV system are about 49% and 24% of the total block area, respectively.

The soil under PV panels was prepared and ploughed with raised beds of 7 cm^2 (7 x 1 m), as seen in Fig. 3.2.

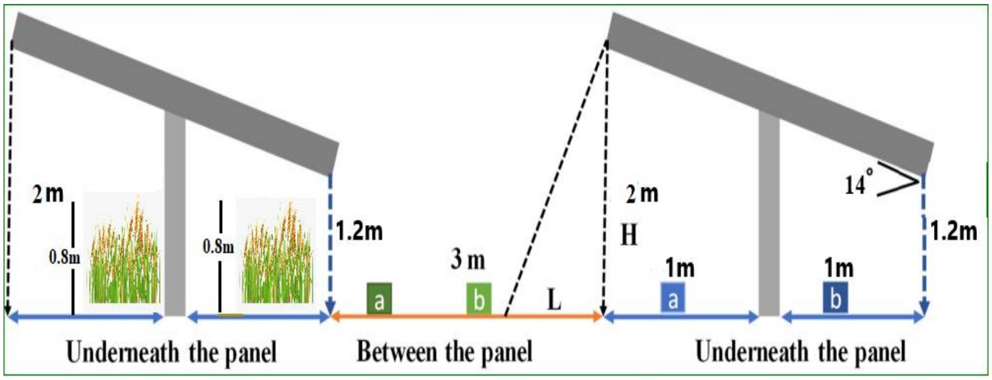

Fig.3.2 Design of AV System

The number of PV modules in the basic AV shed is

$$24\ \frac{PV\ modules}{Supporting\ structure} * 16\ \frac{Supporting\ structures}{Basic\ AV\ shed} \tag{3.1}$$

= 384 PV modules/Basic AV shed

The corresponding peak power is

$$384\ \frac{PV\ modules}{Basic\ AV\ shed} * 400\ \frac{Wp}{PV\ module} \tag{3.2}$$

= 153.6 kWp/Basic AV shed

To calculate the ground area covered by the basic AV shed, we have to multiply its overall width (19 m (Figure 3. 2)) by its overall length. The latter, in turn, is the sum of 45 m (15 × 3 m, Figure 2) plus 1.9 m (the horizontal projection of the last module row cantilever 1.956 m to an angle of 14^0) plus 3 m, i.e., 50 m. Hence, 19 m × 35 m = 950 m^2 = 0.095 ha

To calculate the ground coverage ratio (GCR), the overall module surface area has to be first computed as:

$$384\ \text{PV modules} * \frac{1.956\ m * 0.992 m}{\text{PV module}}$$

= 745 m^2

Then, the GCR is

745 m^2/950 m^2 = 0.784

Power density is

153.6 kWp/0.095 ha = 1616.84 kWp/ha

Considering an effective land area of 1.6 ha, obtained by reducing by 2% the size of the agricultural unit plot to account for mismatch between plot legal boundaries and AV shed orientation, the PV capacity installed in a plots is

1616.84 kWp/ha * 1.6 ha/plot = 2587 kWp/plot

The inverter considered is the SMA SHP Peak 3, which features a nominal AC power of 200 kW [22]. The number of inverters in the agricultural unit plot would be

$$\frac{2587\ kWp/agricutural\ unit}{153.6\ kWp/inverter}$$

= 17 inverters /agricultural unit

The AV system is expected to last 25 years, which is the typical lifespan of PV modules. The inverters have a 13-year service life, which means they will need to be replaced in year 14. Module deterioration was calculated using a degradation coefficient that was set to 1 until year 11 and then lowered by 0.5 percent annually from year 12 onwards.

3.3 Solar water pumping system sizing: A Case Study

The system comprises a stand-alone 153 kWp solar photovoltaic array, inverter, AC motor, and pump set, which can discharge a maximum of 2400 m^3 of water per day. For the pumping system, MATLAB simulation is performed with only energy storage system as potential energy in a large water tank. This energy storage system requires a boost converter and a large water tank to store around 2,400 m^3 of water, which is less costly solution as compared to battery bank energy storage system. This systems yields an efficient and economical solution.

The steps used in designing and selecting solar water pumping system are summarized as follows:

1. During a site visit:

a. Determined the water source and, based on the characteristics of the water source and the water's end usage, selected the appropriate solar water pumping system to be installed.

b. Determined the daily and weekly water requirement and verified that the water resource availability over the long term could meet the requirements.

c. Determined where the solar array is located.

d. Determined where the water pump is located.

e. Determined the length of cables required between the solar array, pump controller and water pump.

f. Determined where and how the water is to be stored.

g. Measured the static head for the site.

h. Measured the total distance from the water source to the final location of the water.

i. Determined and measured land irregularities (hills, ditches, etc.) that the piping system must traverse.

2. Determined the solar irradiation for the selected site on an annual and a monthly basis.

3. Selected the size and type of the water pipe to be used to transfer the water from the source to its storage tank.

4. Made an estimation of the expected dynamic head and select a possible solar water pumping system using manufacturers' tables accounting for available solar irradiation. This is then provided information on the maximum flow rate.

5. The dynamic head is determined by the estimated maximum flow rate and calculated the frictional losses (flow friction head)

6. Chosen a type of pump consistent with the quality of the water being pumped and the overall characteristics of the site.

7. With the final calculated dynamic head finalized, the solar water pumping system from manufacturer tables selected.

3.3.1 Water resource

The company who prepared the borehole/well has undertaken tests to determine the maximum flow possible from the borehole or well. So we obtained this information from the company who developed the water source. This information is generally provided with average discharge of 342 cubic meters per hour.

When selecting the solar water pumping system, it is ensured that the system does not have a maximum flow rate greater than the borehole can provide. The volume of water pumped by a solar water pumping system varies throughout the day because the available solar power (irradiance) varies throughout the day. This results in the maximum flow rate possible from the borehole pump only being achieved when the solar power (irradiance) is at its highest value during the day and also means that there will be no water pumped after sunset and before sunrise.

There may be times, because of this maximum flow rate possible from the borehole and the fact that the solar water pumping system can only provide a specified total volume of water over a day, that a system cannot be selected to meet the total daily water volume required. To overcome such difficulty batteries are included to allow the water to be pumped more slowly and more evenly over more hours of the day. During the periods of lower solar power (irradiance) the system will be pumping less than the maximum flow rate of the borehole but still more than the possible flow from the pump. For the periods when the available solar power results in a pumped flow rate greater than that possible from the borehole, it is included in the system installation a set of water sensors which turn the water pump off when the water falls below the level of the intake of the pump. It will restart when the source refills. It is designed that the sensors such that there is not an excessively rapid cycling of the pump.

In this case study, a well with 30 m depth is the water source but the pump level was selected to be on a depth of 27.5 m. 2.5 meters were left to accumulate water underground, avoiding pump damage from any sands or stones.

Determination of water need

Parameters used for head calculation are given in the table below Table

Table 3.2: Head calculation

Parameter/Project	**Sheder**
I) Given Parameters	
Coordinates	9.66N,43.12E
Borehole elevation (m)	677
Tank elevation above borehole head (m)	6
Borehole depth (m)	30
Casing Diameter (mm)	203.2
Casing type	Pvc
Safe yeild(L/s)	1.6
SWL(M)	16.05
DWL(M)	26.8
Pump position @ safe yield (m)	27.5
Type of riser pipe	GI
Size of riser (mm)	101.6
Desired discharge (m^3/day)	2400
Length of pipe line(m) from borehole head to tank	50

Type of pipe (Borehole to reservoir)	HDPE
Size of pipe (mm) (Borehole to reservoir)	101.6
Residual Pressure	9

From the given parameters, the following values are calculated

Safe yield in m^3/hr = safe yield (L/s) * 3.6 = 1.6 * 3.6 = 5.8

3.3.2 Desired discharge

A daily water demand has been projected to irrigate an average farm which contains more than 80 hectares cash crops. According to a study conducted in the gulf region show that the average daily water consumption for each hectare of Wheat is 30 m^3/day. Consequently, the total daily consumption of the whole farm can be obtained from the below expression.

$$Area\ to\ be\ irrigated\ \times\ Consumed\ water\ per\ hectare \tag{3.3}$$

80 ha * 30 m^3 / day = 2400 m^3/day.

The water demand is not fixed every day but there is fluctuation happens on a seasonal basis. Assuming 7hr sun shine,

$$Desired\ discharge\ =\ \frac{Desired\ discharge\frac{m3}{day}}{peak\ sun\ hour\left(\frac{h}{day}\right)} \tag{3.4}$$

= 2400/7 = 342.8 m^3/h

3.3.3 Static Head

Static Head is the sum of Dynamic Water Level (DWL) to Borehole Surface [m] and Borehole Surface to Reservoir [m]

From the above table DWL to Borehole Surface is 26.8 m

Static Head - Borehole Surface to Reservoir [m] = height of reservoir + elevation difference between borehole

= 6m + 16m = 22 m

Static Head = 26.8m + 22m = 48.8 m

3.3.4 Dynamic Head

Dynamic Head is the sum of Dynamic Head - GI Riser Pipe [m] and Dynamic Head - Transmission Line [m]

Dynamic Head - GI Riser Pipe is calculated as

$$10.67\left[\frac{\text{pump position}}{\left(\frac{\text{size of riser pipe}}{1000}\right)^{4.87}}\right]\left[\left(\frac{\frac{\text{desireddischarge}}{3600}}{\text{Hazen William GI pipe coefficient}}\right)^{1.852}\right]$$

$$10.67 * \left[\frac{27.5}{\left(\frac{152.4}{1000}\right)^{4.87}}\right] * \left[\frac{\frac{342.85}{3600}}{120}\right]^{1.852} \quad = 5\text{ m}$$

Similarly, Dynamic Head - Transmission Line is

$$10.67\left[\frac{\text{Pipe length(m)}}{\left(\frac{\textit{Borehole to reservoir}}{1000}\right)^{4.87}}\right]\left[\left(\frac{\frac{\textit{desireddischarge}}{3600}}{\textit{Hazen William HDPE pipe coefficient}}\right)^{1.852}\right]$$

$$10.67 * \left[\frac{200}{\left(\frac{152.4}{1000}\right)^{4.87}}\right] * \left[\frac{\frac{342.85}{3600}}{14\ 0}\right]^{1.852} \quad = 27\text{ m}$$

Dynamic Head = 5 + 27 = 32 m

Total Head of pump (T. Dynamic + T. Static) [m] = Static Head + Dynamic Head + Residual Pressure = 48.8 + 32 = 80.8 m

Minimum PN rating of riser Pipe [Bar] = Total Head of pump/10 = 80.8/10 = 8.08 bar

Minimum PN rating of transmission Pipe [Bar] = (Borehole Surface to Reservoir + Dynamic Head)/10 = (22+3)/10 = 2.5 bar

3.3.5 Pump Sizing

There are several strategies that have been followed to select the best or the optimized system. One of these methods is using Homer software along with some calculation. Homer can be very useful tool when it is utilized with accurate values of PV, converter, batteries and other components' prices and sizes. In this study, all prices and sizes have been selected properly. To start sizing such a system, the pump size is an important aspect that needs to be assessed. As the total head and water demand are known for a farm, the pump size calculation is forthright, and can be completed using the following expression (3.5).

$$Ph = \frac{Þ*g*TDH*Q}{3600*1000} \tag{3.5}$$

$$= \frac{1000*9.8*80.8*342.85}{3600*1000} = 75.4 \text{ kw}$$

TDH is the total dynamic head (m), P_h is hydraulic power (kw), Þ is water density (1000kg/m^3), g is the gravitational constant (9.81m/s^2), Q is the flow rate (m^3/h), and P is shaft power (kW). The total head includes the distance from pump level to the tank as well as the fraction of elbows. As shown earlier, the total head dynamic is 80.8 m and the maximum flow rate is 2400 m^3/day Results from equation show that the calculated pump size is 75.4 kW which can deliver the required amount of water.

Motor Sizing

The induction motor power is

$$Pm = \frac{Ph}{\eta} \tag{3.6}$$

$$= \frac{75.4}{0.85} = 88.7 \text{ kW}$$

For the purpose of simplified design 92 kW is used. η is induction motor-pump efficiency and assumed as 85%

From the above calculations we are supposed to select our submersible pump that will deliver 342.85 m^3/h to a water tank with TDH 80.8 m and 75.4 kW, the Grundfos SP 215-5 - 18A55605 pump, which uses the performance curves of Grundfos (as shown in Figure 3.3), has been chosen. This submersible borehole pump is suitable for pumping clean water and can be installed vertically or horizontally. All of its steel components are stainless steel, EN 1.4301 (AISI 304), which ensures high corrosive resistance. The pump also carries drinking water approval and is fitted with a 92 kW MMS8000 motor with sand shield, mechanical shaft seal, water-lubricated journal bearings, and a volume-compensating diaphragm. The motor is a canned-type submersible motor that offers good mechanical stability and high efficiency, and is suitable for temperatures up to 40˚C.

Table 3.3: Characteristics of the motor

Parameter	Value
Rated power	92 kW

Rated voltage	3 x 380 V
Rated current	194 A
Rated speed	2870 rpm
Starting Method	star/delta
Mains frequency	50 Hz

Figure 3.3a demonstrates the motor curves, efficiency, power factor, current, shaft power, and shaft speed of the motor. The current, power factor, shaft speed and efficiency of the motor were found to be 79.8%, respectively.

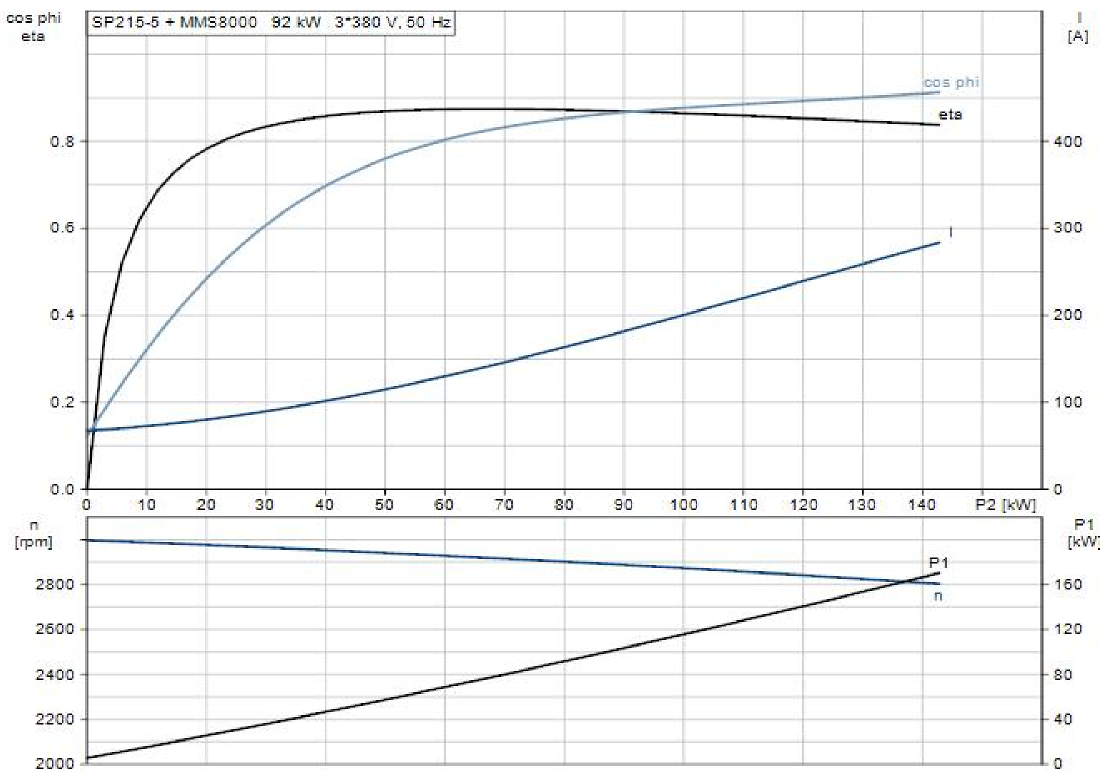

Figure 3.3a: Motor performance Curves

Figure 3.3b shows the system curve, pump curve, NPSH curve and efficiency curves. The system curve has the pump curve as the operating point of pump chosen for the TDH and flow rate. The given values of TDH= 80.5 m and Q = 342 m^3/h are shown for the motor power P1 =153 kW and the shaft power P2 = 145 kW, respectively. From the above values, the efficiency of the pump was calculated as 80%, while the total efficiency of the system was 56%.

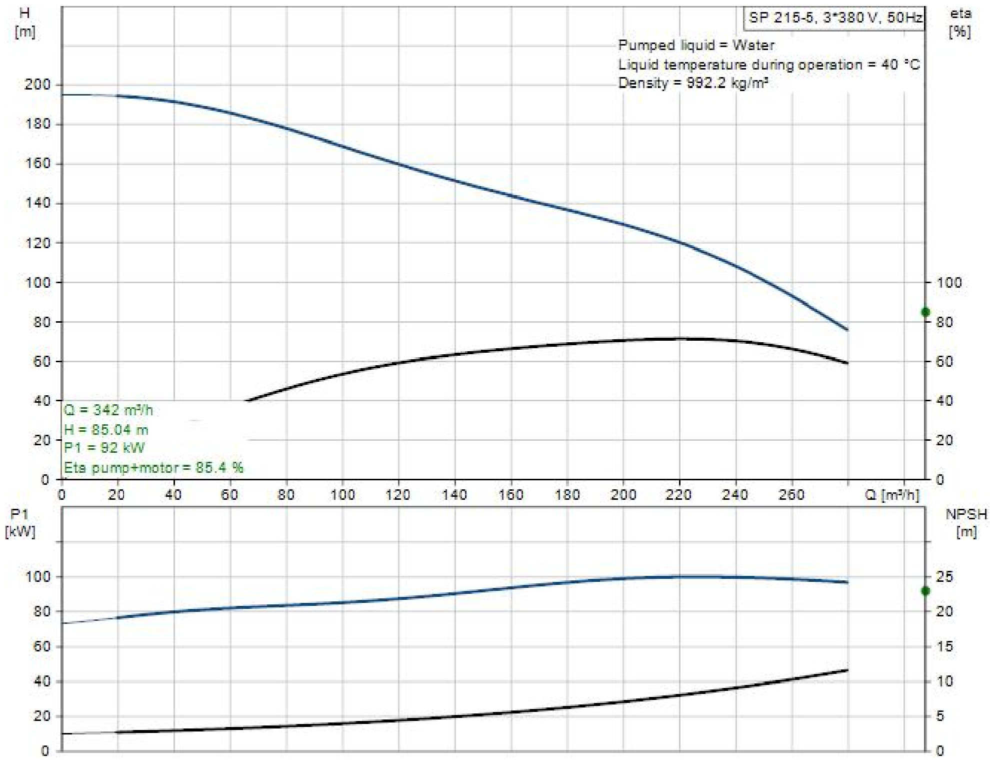

Figure 3.3b: Pump performance Curves

The matlab design of motor pump is shown in the figure below

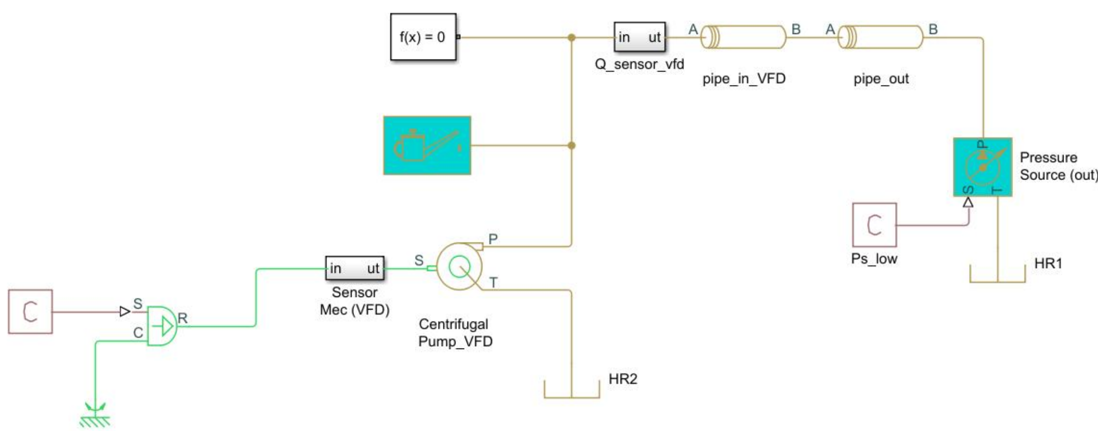

Figure 3.4: Simscape model of motor pump

Fig. 3.5 presents the torque, power, and speed shaft of the pump calculations in MATLAB/SIMULINK model.

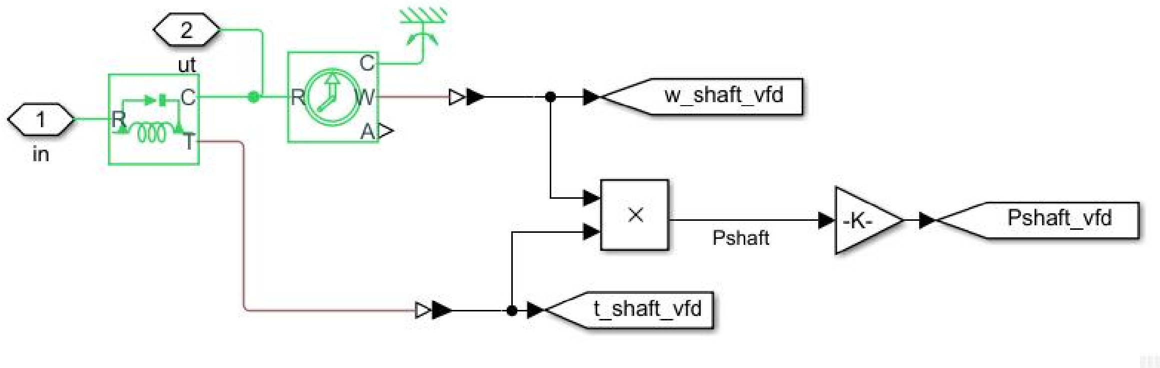

Figure 3.5: Sensor calculation in model.

3.3.6 PV Panel

The system is designed to run for only eight hours during day time (8 a.m.–4 p.m.).

Pump use = (92 kW × 8 h) = 736 kWh/day. To estimate the needed PV energy, the total watt-hour per day is divided by the mismatch factor. The recommended standard mismatch factor is 60 to 70 percent. For this system, 60% is selected. Assume this mismatch factor includes the losses that occur during power conversions between the load and the PV panel. Therefore,

$PV\ energy\ needed\ = \frac{736000}{0.6}$ = 1,226,666.67 Wh / day

To get the desired power of the system, divide the PV energy needed by the working hour per day.

$$PV\ power\ needed\ = \frac{PV\ energy\ needed}{Working\ hour\ per\ day} \tag{3.7}$$

$$= \frac{1,226,666.67}{8} = 153.33 \text{ kW/day}$$

For this research work, PV panel with 400W_P is selected based on load design, availability, and cost. Therefore,

$$Number\ of\ modules\ = \frac{PV\ array\ size}{Rating\ power\ per\ module} \tag{3.8}$$

= 153333 / 400 = 384 modules

The selected panel is 144 cell panels and number of panels connected in series in each string is two. As a result, the bus voltage is 48 V.

Table 3.4: Technical specification of solar PV module

Parameter	Lowercase
Cell material	Mono Crystalline silicon
Nominal power of each PV module [Wp]	400+ 3%
Power model	Only temperature effect
Coefficient of variation of power with temperature - g [%/ C]	0.420
Nominal operating cell temperature e NOCT [ºC]	45
Power Sorting [W]	0~ 4.99
Voltage at Pmax [V]	41.7
Caurrent at Pmax [A]	9.60
Open-Circuit voltage Voc [V]	49.7
Short-Circuit Current Isc [A]	10.06
Maximum System Voltage [V]	DC 1000
Maximum Series Fuse Rating [A]	20
Mechanical Load Test [Pa]	5400
Weight [Kg]	21.5
Dimension [mm]	1956*992*34
Safety Application Class	Class A
All technical standard test condition	AM=1.5 E=1000W/m2 Tc=25ºc
Operating(Nominal) Voltage	24
Solar Panel Type	Monocrystalline
Temp.Coeff.of Isc(TK Isc)	0.049%/℃
Temp.Coeff.of Voc(TK Voc)	-0.26%/℃
Temp.Coeff.of Pmax(TK Pmax)	-0.34%/℃
Operating temperature	-40~+85℃
Normal operating cell temperature	45±2℃

The number of modules that need to be connected in parallel and series (the string) is determined based on the module's operating output current and voltage characteristics. Series connection of modules increases the total voltage (as a multiple of the number of series connected modules) to match or exceed the voltage input required by the inverter. Next, the PV string (series connected group of modules) is connected in parallel to increase the total current and power available from the modules to match or exceed that required by the inverter.

$$Number\ of\ modules\ in\ series\ = \frac{pump\ inverter\ voltage}{Voc} \tag{3.9}$$

$$= \frac{1000V}{4\ 17V}$$ = 24 series connected modules

Number of modules in parallel:

$$Np\ = \frac{total\ number\ of\ Modules}{Series\ connected\ strings} \tag{3.10}$$

$$Np\ = \frac{384}{24} =\ 16$$

.Nt = Np * Ns = 16*24 = 384 modules

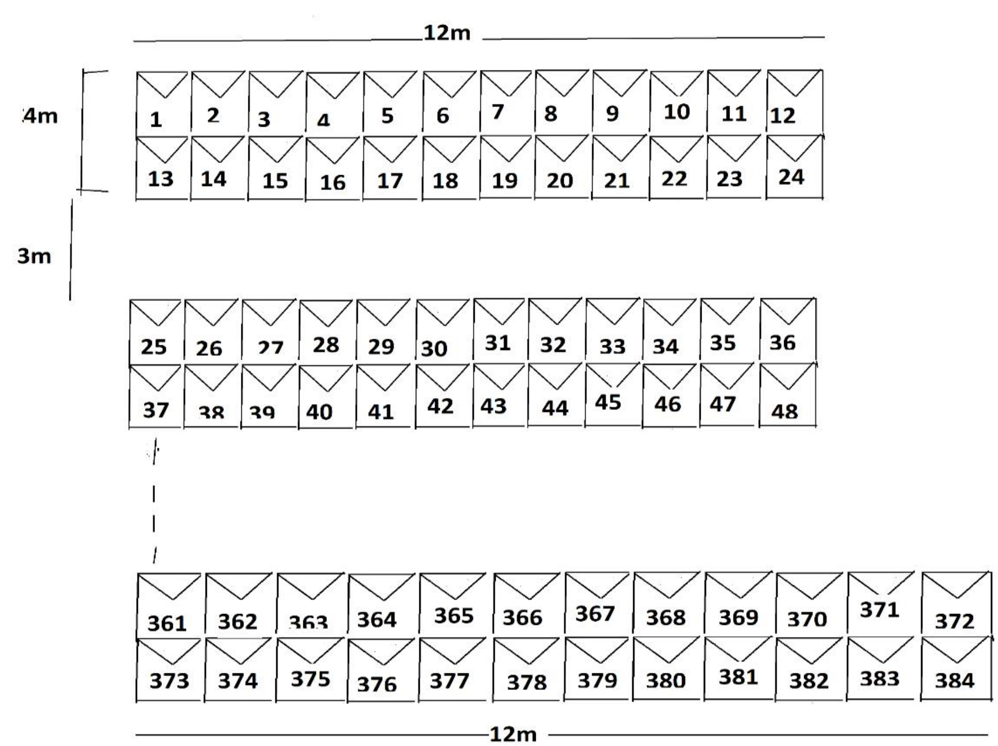

Figure 3.6: Number of PV array

3.3.7 Sizing of the Inverter

Before sizing the inverter the actual power drawn from the appliances that will work at the same time first determined. The inverter capacity is selected as 132 kW (40% bigger than the motor size).

For a DC input voltage of 120 V_{DC} series connected inverter output is 380 VAC.

Table 3.5: Technical specification of solar inverter

Parameters	Values
Rated power	132 kW
Mains frequency	50 Hz
Rated voltage	380 V
Rated voltage output AC	380 V
Voltage input DC	800 V
Rated current output AC	261 A
Vdc	400 V
Enclosure class (IEC 34-5)	IP54
Efficiency	90%
Manufacturer	

3.3.8 Water storage tank sizing

Use of large water storage can reduce the extra cost paid for electric battery which is used as backup energy. When solar intensity becomes low during cloudy weather condition but large water storage stores enough water during peak energy production and it meet the water requirement in case of cloudy weather condition. The proposed tank must store the water at least for a minimum of one day by considering the storage neatness in order to prevent water-borne diseases.

Same period of time in the battery sizing is applied on the water storage tank. It was assumed that the absence of lighting or the cloudy day is only one day. Thus, the size of tank is going to be estimated as:

Proper tank size = Number of the cloudy days * the average amount of water= 1* 2400 m^3/day = 2400 m^3

Therefore, if the height of the tank was already known, which is 6 is shown below in the layout.

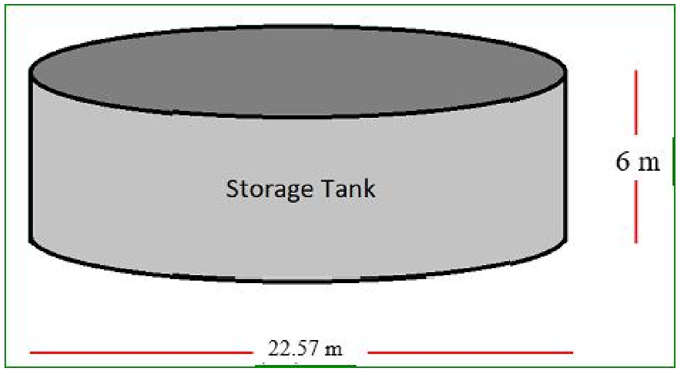

Figure 3.7: 2400 m^3 capacity water storage tank

The cost of the tank is much cheaper than batteries; the estimation is provided below with some details. The tank is made from concrete which is the common type for irrigation in Afar region. The tank is a cylinder shape based as shown in figure 3.7 same as estimated in expression 3.11.

$$V = \pi * r^2 * h \tag{3.11}$$

where V: volume in m^3, r: radius in m, h: height in m

$V = 11.285^2 * 6 * \pi = 2400\ m^3$

In the estimated water demand, the pump will work for 8 hours each day pumping at the specified discharge and it needs 92 kw x 8 hours x 1days = 736 kWh energy is required for the storage capacity of the tank. The storage tank need controller (float switch) which is used when the water volume is above the tank level limit then the pressure switch controls the pump operation. In Ethiopia, such a tank costs around 316,850 Br which is reasonable price for a very large tank. Yet it is highly recommended instead of batteries.

Figure.3.8 gives an overview about hourly water discharge rate of this site.

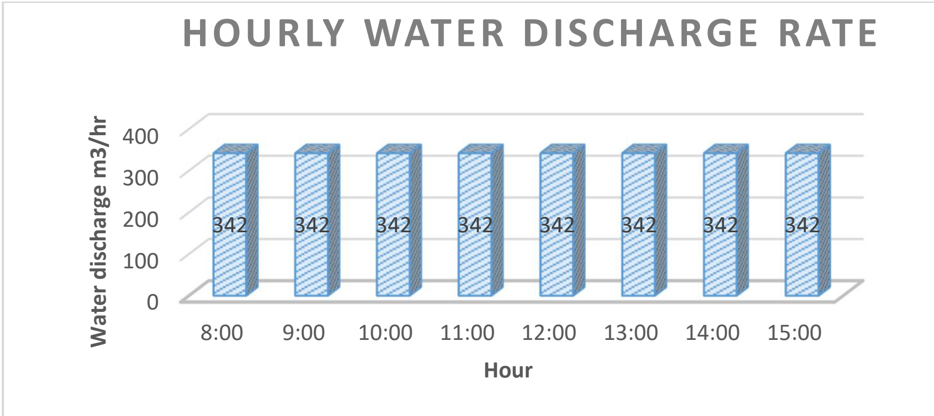

Figure 3.8: Hourly water discharge rate

Figure below demonstrates Overall solar water pumping system based on a water tank.

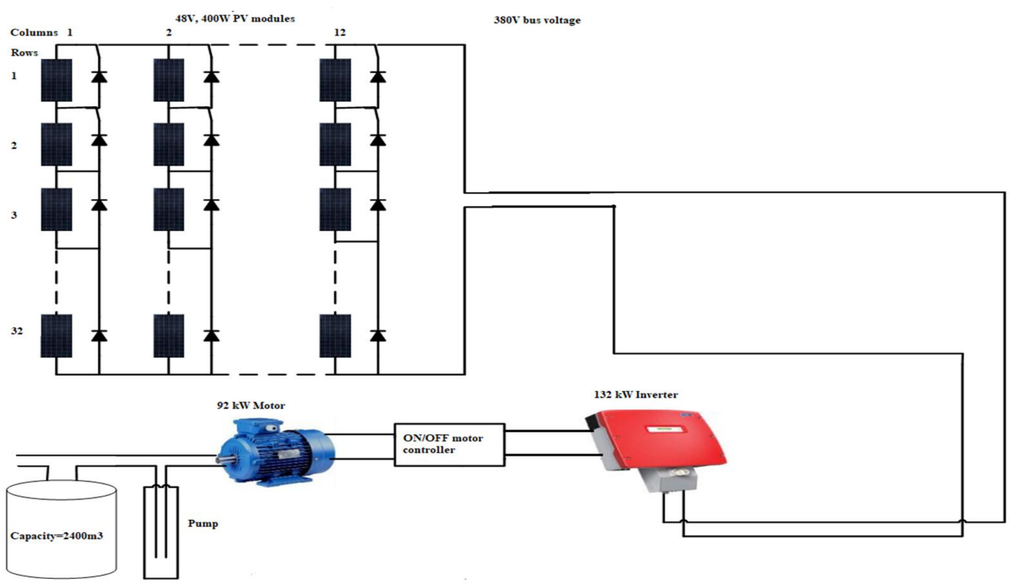

Figure 3.9: Overall solar water pumping system.

3.4 Power System

The PV modules, MPPT- charge controller, batteries and induction motor are the components, which make up the power subsystem of this AV system. The working mechanisms and specifications of these devices are discussed in this section.

3.4.1 Solar Panels

The system uses two ND-224UC1 PV modules manufactured by the Sharp Electronics Corporation and are shown in Figure. Each module measures 1956*992*34 meters and consists of 144 monocrystalline silicon cells connected in series, which can produce maximum power

(Pmax) of 400 watts at standard test conditions (STC). STC refers to standard test conditions for PV modules which are 25° C, 1000 watts- m^2 of solar insolation and a non-dimensional air mass (AM) of 1.5. It is important to note that operating temperatures of these PV modules are usually higher than 25° C; at higher temperatures than 25° C PV panels produce less than their rated power output at a solar insolation of 1000 watts-m^{-2} and their efficiency drops due to this temperature affect.

Figure 3.10 : Photovoltaic modules used in the AV system.

In the installation 16 modules are connected in parallel 24 modules are connected serially via multiple contact locking connectors, MC4 connectors, to maintain approximately 28 volts. So that the performance of each individual PV panel can be measured, the individual positive side wires from each panel run through current sensors and are linked together before they are connected to the MPPT charge controller. Similarly, negative wires from the panels are also linked together via MC4 connectors, but they are connected right after the panels' outlet. Subsequently, positive and negative wires from the PV array are connected to relevant terminals of the MPPT controller.

Serial configuration

In this case, all the photovoltaic energy produced passes through the battery bank, is converted from DC to AC by the inverter, and then transferred to the AC load (Fig. 3.11).

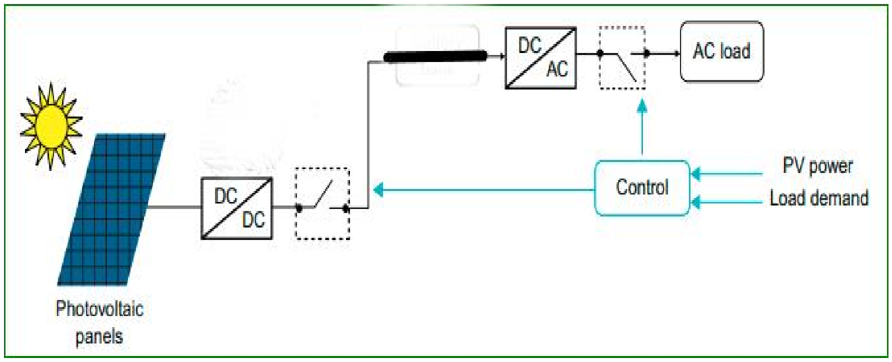

Figure 3.11: Serial architecture for photovoltaic installations.

Parallel configuration

The parallel configuration allows all energy sources to supply the AC load separately (Fig. 3.12). Moreover, a reduction in the rated inverter, and photovoltaic panel is feasible, while also meeting the demanded load peaks and ensuring the installation autonomy.

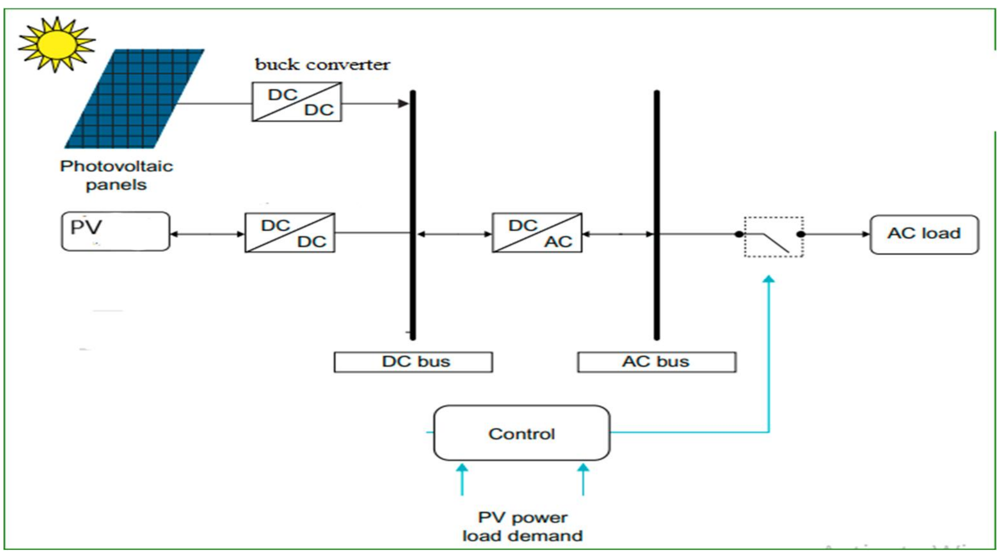

Figure 3.12: Parallel architecture for photovoltaic installations

V-I characteristics and the power curve have been simulated in MATLAB. The following Figures 3.13 describe the V-I characteristics and the power curve of PV array.

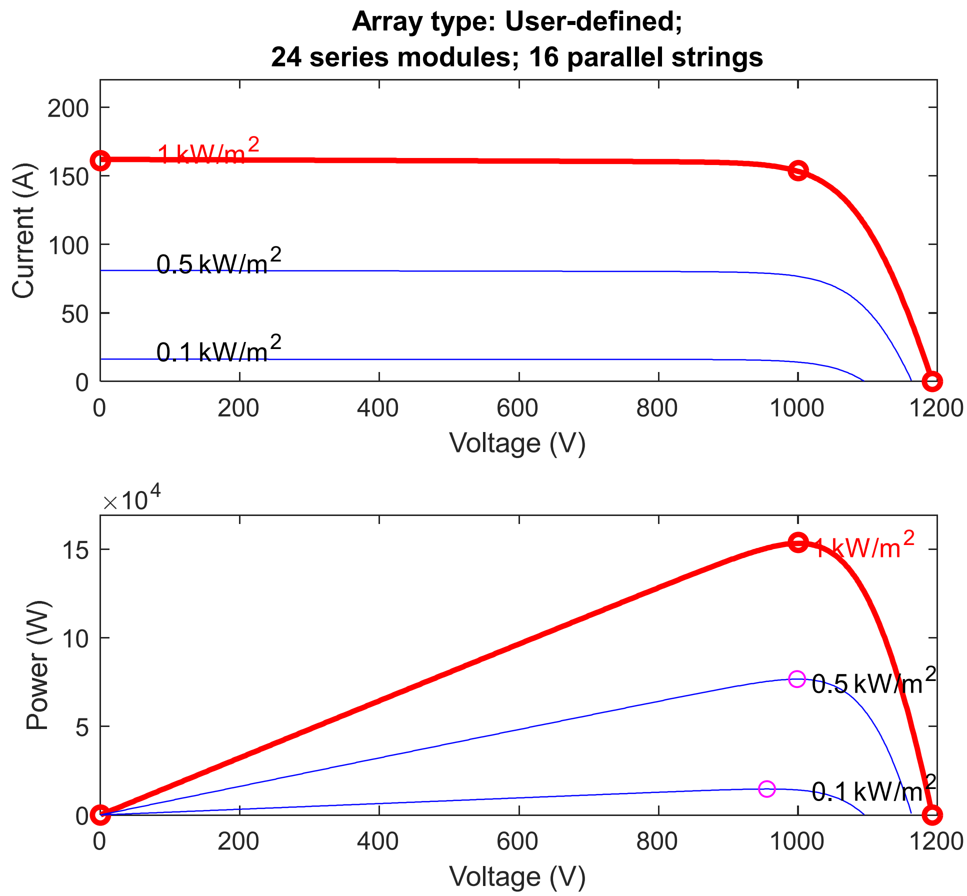

Figure 3.13: PV array I-V and PV curves

3.4.3 DC-DC Buck Converter

A dc-dc buck converter is a dc voltage converter that converts an unregulated dc input to a lower controlled dc output. This transformation is accomplished by the employment of semiconductor devices that operate at high switching frequencies. Because it is a DC-DC converter, it completes the task with a few transistor switches and an inductor. The graphic below depicts a common buck converter circuit.

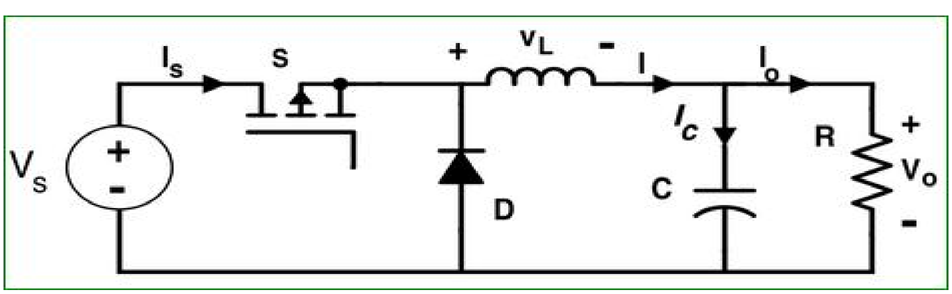

Figure 3.14: Buck Converter Circuit

The buck converter is comprised of a DC supply or a rectified AC output, two switches, D (diode) and S (power electronics switches that can be semi-controlled or fully-controlled), a two-pole low-pass filter (L and C), and a load. Let the duty ratio of switch S be

$$D = \frac{T_{on}}{T} \tag{3.12}$$

Where

$T = T_{ON} + T_{OFF}$

The switch shown in the above circuit is normally a power electronics switch IGBT. The switch is switched (turned on and off) by using a PWM signal.

Working of a Buck Converter

This circuit can be investigated in two ways. The first mode occurs when the switch S is turned off, while the second mode occurs when the switch S is turned on.

$$\text{Voltage across the Inductor, } V_L = L\frac{dI}{dt} \tag{3.13}$$

Where $I = I_C + I_O$

$$\text{Load Current, } I_0 = \frac{V_0}{R} \tag{3.14}$$

Mode – 1: When the switch S is ON

The switch is activated, allowing electricity to flow to the output capacitor, charging it. The voltage across the capacitor during the switching cycle is not the entire voltage of the power source since the voltage across the capacitor cannot rise immediately and the inductor restricts the charging current.

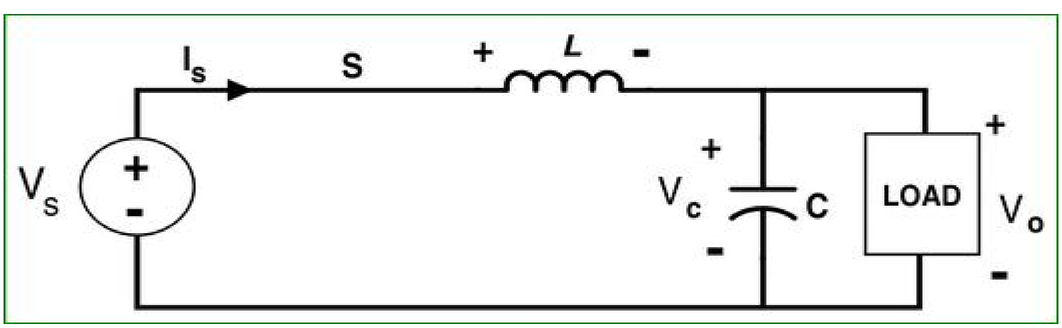

Figure 3.15: when switch S is on (Mode-I)

When the switch S is on and applying the Kirchhoff's voltage law (KVL), we can get,

$$V_S = V_L + V_O \tag{3.15}$$

$$\Rightarrow V_s = L\frac{dI}{dt} + Vo \text{ and } V_O = V_C$$

Mode – 2: When the switch S is OFF

The switch has now been turned off. Because an inductor's current cannot vary abruptly, the inductor generates a voltage across it. When the switch is switched off, this voltage is permitted to charge the capacitor and power the load via the diode, sustaining current output current throughout the switching cycle.

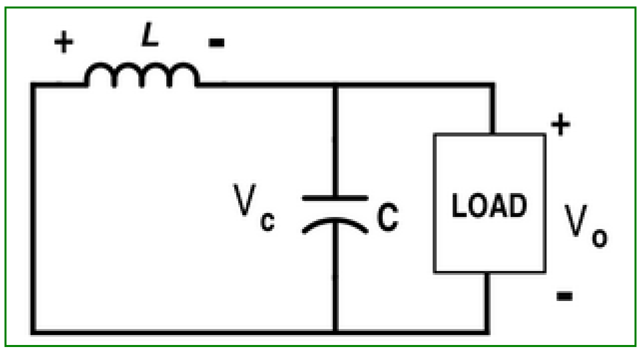

Figure 3.16: Buck converter circuit when switch S is off

When the switch S is off, the KVL in Fig.3.16 gives,

$$V_L + V_O = 0$$

$$\Rightarrow V_o = -L\frac{dI}{dt} \tag{3.16}$$

When the switch is turned off, the diode gets forward-biased to transport the inductor current. When the switch is open, the voltage across the inductor is computed as follows;

$$V_L = -Vo = L\frac{dI_L}{dt} \tag{3.17}$$

$$(\Delta il)open = -(\frac{Vo}{L})(1 - D)T \tag{3.18}$$

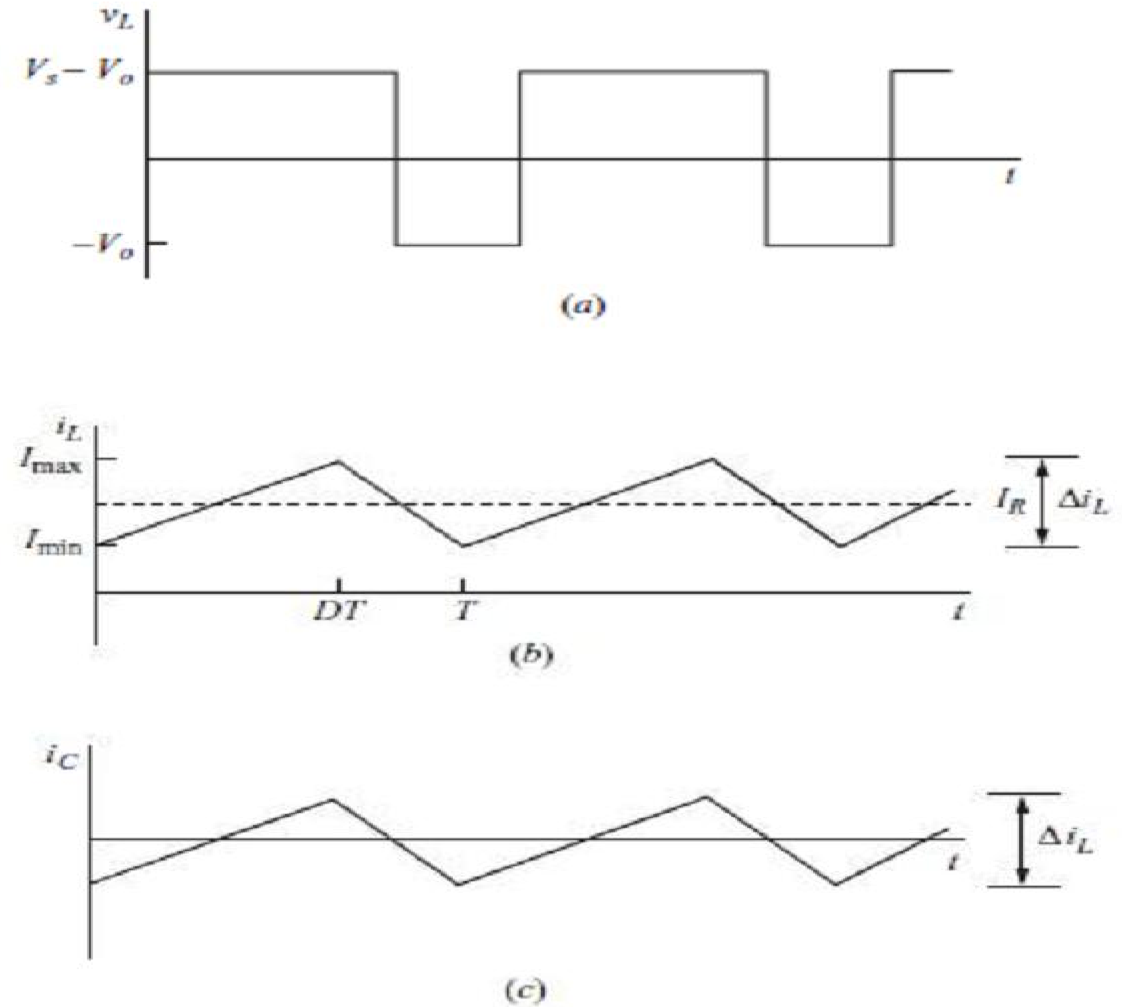

Figure 3.17: Buck converter waveforms (a) inductor voltage, (b) inductor current (c) capacitor current.

Steady-state operation needs that the inductor current at the end of the switching cycle be the same as it was at the start, implying that the net change in inductor current throughout a period is zero. This requires

$$\Delta I_L \text{ (t) closed} + \Delta I_L \text{ (t) open} = 0 \tag{3.19}$$

$$\frac{Vs - Vo}{L(DT)} - \left(\frac{Vo}{L}\right)(1 - D)T = 0 \tag{3.20}$$

Solving for Vo,

$$V_o = V_S D \tag{3.21}$$

The output voltage depends on only the input and the duty ratio D. If the input voltage varies, the output voltage can be adjusted by regulating the duty ratio appropriately. Because the average capacitor current must be zero for steady-state operation, the average inductor current must be the same as the average current in the load resistor.

$$I_L = I_R = \frac{V_o}{R} \tag{3.22}$$

The maximum and minimum values of the inductor current are computed as:

$$I_{max} = i_L + \frac{\Delta i_L}{2} \tag{3.23}$$

$$\frac{V_o}{R} + \frac{1}{2}\left[\frac{V_o(1-D)T}{L}\right] = V_o\left(\frac{1}{R} + \frac{1-D}{2Lf}\right) \tag{3.24}$$

$$I_{min} = i_L - \frac{\Delta i_L}{2} \tag{3.25}$$

$$\frac{V_o}{R} - \frac{1}{2}\left[\frac{V_o(1-D)T}{L}\right] = V_o\left(\frac{1}{R} - \frac{1-D}{2Lf}\right) \tag{3.26}$$

Where, $f = \frac{1}{T}$ is the switching frequency.

To be valid the above equation (3.24), continuous current in the inductor must be verified. Since the minimum value of inductor current must be positive for continuous current. $I_{min} = 0$ is the boundary between the continuous and discontinuous current

$$I_{min} = 0 = V_o\left(\frac{1}{R} - \frac{1-D}{2Lf}\right) \tag{3.27}$$

$$L_{min} = \left(\frac{1-D}{2Lf}\right)R\text{, for continuous current} \tag{3.28}$$

Where: L is the minimum inductance required for continuous current. In reality, an inductance value greater than L is preferable to provide continuous current. To calculate the inductance for a given peak-to-peak inductor current in continuous current operation:

$$L = \left(\frac{V_s - V_o}{\Delta I_L f}\right) D = V_o\left(\frac{1-D}{\Delta I_L f}\right) \tag{3.29}$$

$$\Delta I_L = \left(\frac{V_s - V_o}{L}\right) DT = \left(\frac{V_s - V_o}{Lf}\right) D = V_o\left(\frac{1-D}{Lf}\right) \quad (3.30)$$

Output Voltage Ripple: In this analysis, the capacitor was considered to be quite large in order to maintain a constant output voltage. The change in output voltage, or ripple, is calculated using the capacitor's voltage-current relationship.

The current in the capacitor is $I_c = I_L - I_R$ (3.31)

While the capacitor current is positive, the capacitor is changing.

From the definition of capacitance,

$$Q = CV_o \quad (3.32)$$

$$\Delta Q = C\Delta V_o, \quad (3.33)$$

$$\Delta V_o = \frac{\Delta Q}{C}$$

The change in charge ΔQ is the area of the triangle

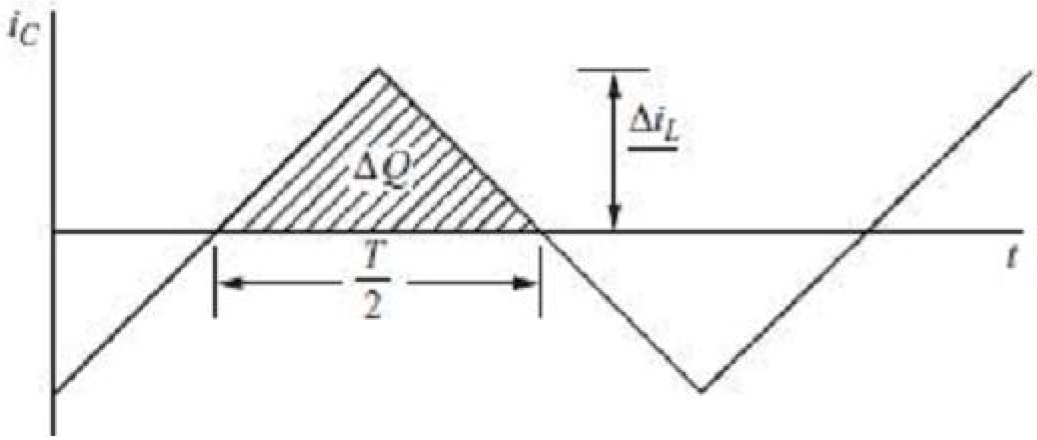

Figure 3.18: buck converter waveform: capacitor current

$$\Delta V_o = \frac{1}{2}\left(\frac{T}{2}\right)\left(\frac{\Delta i_L}{2}\right) = T\Delta I_L\frac{1}{8C} \quad (3.34)$$

$$\Delta V_o = \frac{TV_0}{8CL(1-D)T} = \frac{V_0(1-D)}{8CLf^2} \quad (3.35)$$

The capacitance required is obtained in terms of the specified ripple voltage.

$$C = \frac{1-D}{8L\left(\frac{\Delta V_0}{V_0}\right)f^2} \quad (3.36)$$

Where: $\frac{\Delta V_0}{V_0}$ is equal to $\frac{1-D}{8CLf^2}$, T is the period. The input voltage for the buck converter is 1000V which is obtained from the photovoltaic PV and the required inverter input is buck converter output, which is 380V_{DC}.

The designed Buck converter calculation is computed as follows: Input voltage 1000V, output Voltage, 380V, and ripple voltage is 2-5% of input voltage and Ripple current is 20-40% of the input current [49]. For ripple voltage 0.05x1000V = 50V, and ripple current 0.3x153Amps =45.9Amps. Input power 384 solar panel x400W of each panel gives 153.6kW, Output power 92kW, which is the required power to generate the pump.

$$I_R = I_L = \frac{V_o}{R} = \frac{P_{in}}{V_{in}} \tag{3.37}$$

$$I_R = \frac{153.6\text{kW}}{1000V}\ 153.6\ \text{A}$$

$$R = \frac{V_o}{I_L} = \frac{380}{153.6} = 2.474\ \Omega$$

For the IGBT, the switching frequency taken is 10KHz. By comparing equation (3.30) with the calculated output ripple voltage value, 30.4V = $T\Delta I_L\ \frac{1}{8C}$, from this, the capacitor value can be calculated, c = 22µF, L = 113.6mH.

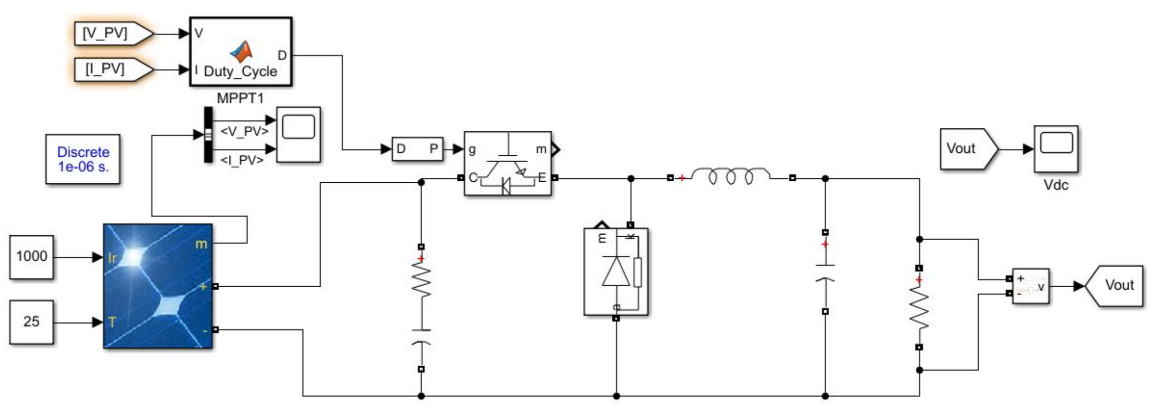

Figure 3.19 MATLAB Simulink Model for Step-down DC- DC Converter

3.4.4 Inverter

The inverter adjusts the output voltage or frequency values of the motor, and controlled by pulse width modulation (PWM) from controller, so that the output current waveform closely approximates a sine wave (quadrature-axis). Electronic power switches (IGBT) Insulated Gate Bipolar Transistor, switch the rectified DC **on** and **off**, and produce a current or voltage waveform at the desired new frequency to controls the motor torque.

System Used For Solar Photovoltaic Power Conversion

Centralized System

It is installed close to the main service panel A centralized system consists of several solar panels that are assembled in series and in parallel to create a solar array. This entire array is fed into a power converter in order to execute the MPPT. An example of a centralized system is seen in Figure 3.20. The dashed lines are intended to indicate that the size of the array can be variable. In other words, one can connect several solar modules in a variety of different series and parallel combinations.

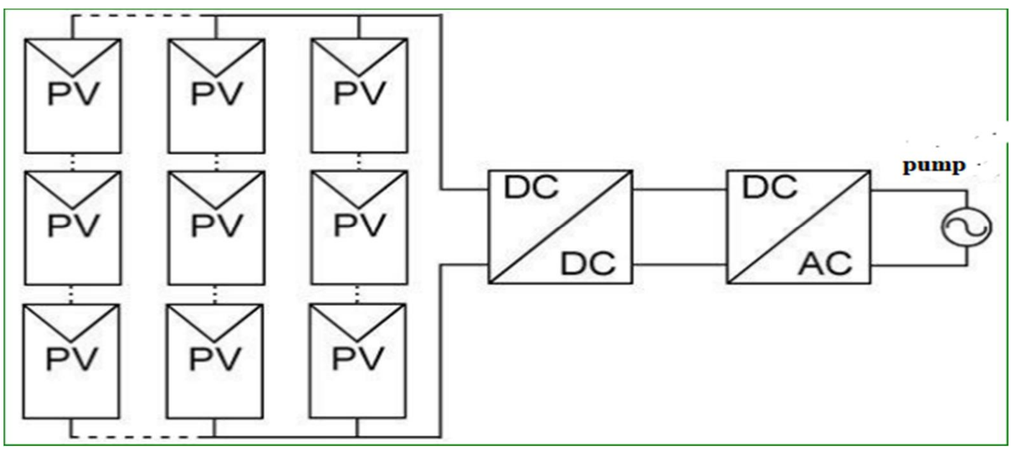

Figure 3.20 Schematic diagram of a centralized system

The system displayed in Figure 3.20 can be referred to as a two-stage topology since it employs two separate power converters. The DC-DC converter conducts bucking the voltage from the array, while the DC-AC inverter allows for the rest of the system to interface with the AC pump. It is important to realize that for all of these systems a single-stage topology, which contains only one DC-AC inverter, can be used as well.

There are several pros and cons of a centralized system. For instance, since this system does the MPPT for the entire array, it cannot account for individual panels that are operating differently; thus, while individual panels may not be operating at their MPP, the array is driven to its MPP. The disadvantage of this construct is that some of the available power is not extracted from the array because each individual panel is not at its MPP. An advantage of this type of system is that the components used to realize such a system are minimized. As one may realize from Fig

20, this type of system uses only a DC-DC converter and a DC-AC inverter for the entire array. There are other topologies which typically uses more power electronic components. Another benefit of using a centralized system is that the control methodology is relatively simple when compared to other systems since it only has to control one or two converters vice multiple converters.

Inverters take care of four basic tasks of power conditioning:

- ✓ Converting the DC power coming from the PV modules or battery bank (if it is there) to AC power
- ✓ Ensuring that the frequency of the AC cycles is 50 cycles per second
- ✓ Reducing voltage fluctuations
- ✓ Ensuring that the shape of the AC wave is appropriate for the application, i.e. a pure sine wave.

Insulated Gate Bipolar Transistor (IGBT) Inverter

An IGBT is used for built-in two-phase DC to three-phase AC conversion, with a PI controlling the pulse.

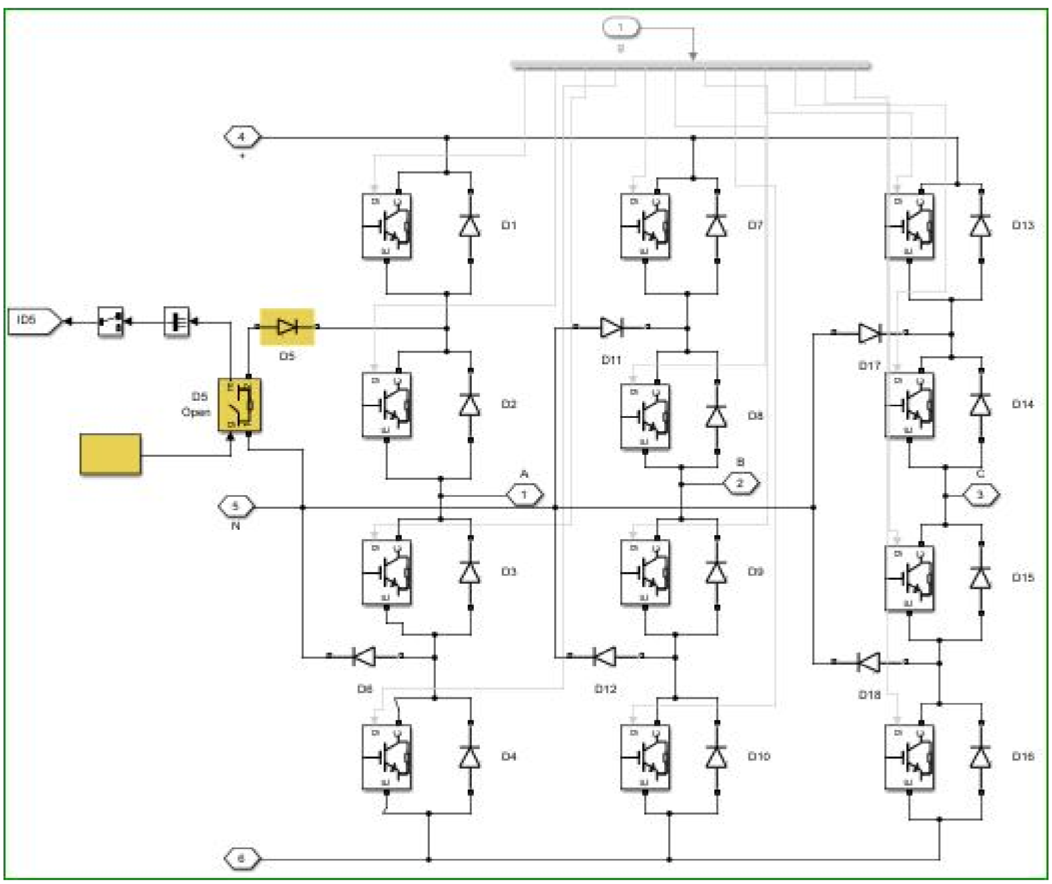

Figure 3.21: Three-Level Inverter (Detailed)

3.4.5 Combiner Box

Wires are extended from individual PV modules or strings to the combiner box, which is normally positioned on the roof. These cables could be single conductor pigtails with pre-wired connectors on the PV modules. The combiner box's output is a single bigger two-wire conductor in conduit. A combiner box will normally have a safety breaker for each string as well as a surge protector.

3.4.6 Surge Protection

Surge protectors help to safeguard our system against power surges caused by a lightning strike on the PV system. A power surge is a large rise in voltage above the design value.

Installation of power meter

Power meter was installed for measure electricity production of the solar power system that is produced in conjunction with agriculture. To compare the efficiency of electricity.

3.4.7 Cable sizing

During star-delta starting, the current will be reduced by √3 (I x 0.58), meaning that the cable length may be longer (L x 1.73). If, for example, the operating current is 10 % lower than the full-load current, the cable may be 10 % longer than indicated in the tables. The calculation of the cable length is based on a maximum voltage drop of 1 % to 3 % of the rated voltage and a water temperature of maximum 30 °C. This is only economical if the borehole provides the necessary space, and if the operational time of the pump is long, especially if the operating voltage is below the rated voltage.

Maximum cable length for a three-phase submersible pump:

$$L = \frac{U * \Delta U}{I * 1.73 * 100 * (\cos\varphi * p/q + \sin\varphi * XL)} \text{ [m]}$$

Where

U = Rated voltage [V]

ΔU = Voltage drop [%]

I = Rated current of the motor [A]

cos φ = Power factor

ρ = Specific resistance: 0.025 [Ω mm^2]

q = Cross-section of submersible drop cable [mm2]

sin φ = √(1 - $\cos^2$ φ)

X_L = Inductive resistance: 0.078 x 10^{-3} [Ω/m].

L = 380 * 3 / 194*1.73*100*(0.88*0.028 +

$$L = \frac{380 * 3}{194 * 1.73 * 100 * (0.88 * 0.025/25 + 0.77 * 0.078 \text{ x } 10 - 3)} \text{ [m]}$$

L = 90 m

For calculation of the power loss in the submersible drop cable, use this formula:

$$\Delta p = \frac{(3\ x\ L\ x\ \rho\ x\ I\hat{}2)}{q}$$

Cable selection

3 x 185 mm^2

$$\Delta p = \frac{(3\ x\ 90\ x\ 0.02\ x\ 194\hat{}2)}{185} = 1098 \text{ W}$$

3.4.8 Grounding Surge Arresters

Above ground surge arresters must be grounded from metal to metal all the way to the lowest draw down water level in order to function properly. Power surges can cause harm if the system is not properly grounded. Surge protection for the motor is provided by grounding the arrester to the supply ground or to a driven ground rod.

Overall System Modeling

The MATLAB/Simulink library blocks were complex, and a system consisting of them would not be suitable for dynamic analysis over long time intervals. In contrast, our goal was to do dynamic analysis on the specified system at regular intervals to comprehensively test it. As a result, the dynamic modeling of the proposed system was done in MATLAB/Simulink utilizing models based on their mathematical equations. The mathematical modeling of many design components allowed for rapid simulation, resulting in a robust design. Figure 3.22 depicts a model of the suggested system.

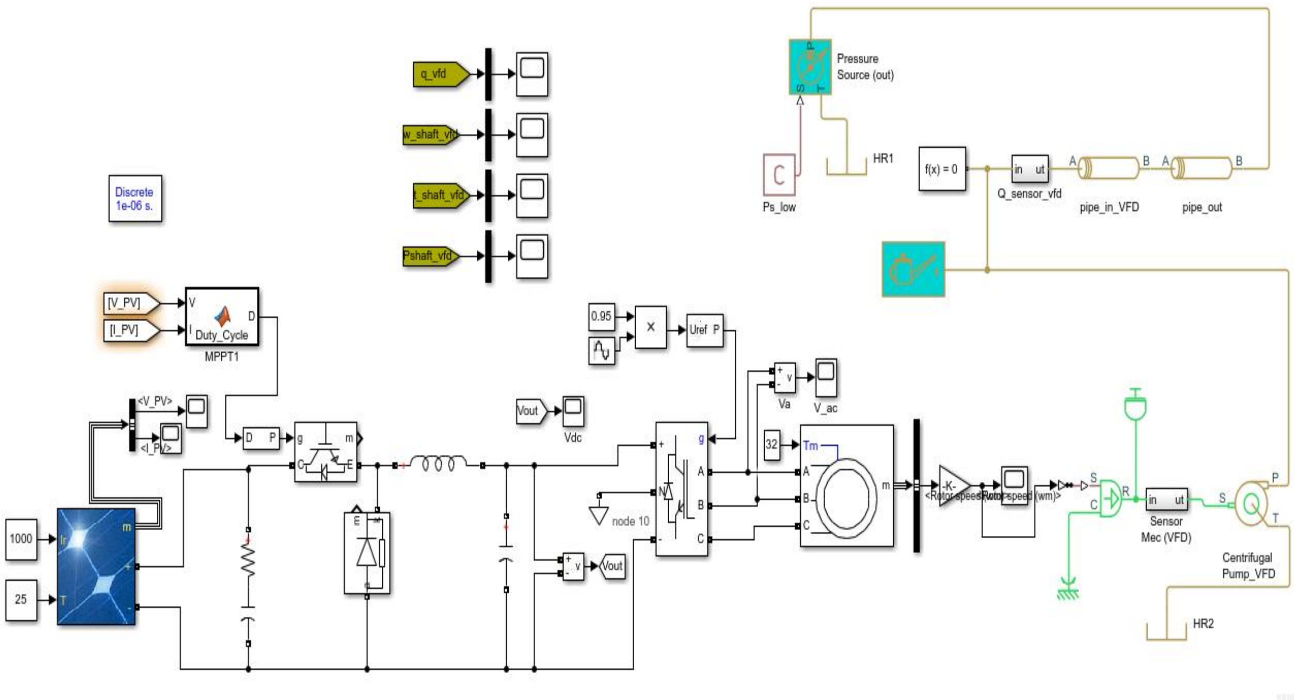

Figure 3.22: MATLAB/Simulink complete model of the proposed system.

3.6 Economic Analysis

The analysis and the estimation of expected benefits of colocation of solar power generation with crop production were based on Life Cycle Cost Analysis (LCCA) of the following land use scenarios: a standalone solar photovoltaic system, standalone cultivation of an "ideal" co-location crop and co-located solar PV-crop system.

LCCA is a concept that is often used to determine the viability of new technologies in which environmental footprints, such as energy and greenhouse gas emissions and water and land usage throughout the life cycle of a technology is estimated (Hsu et al., 2012; Ravi et al., 2016)

Profitability Analysis

To determine the profitability of an AV system, the stream of annual income and expenditure during the project lifetime has to be computed. Expenditure comprise initial investment cost (ascribed to the PV activity, since all the crops considered are annual), plus annual operation and maintenance costs (due to both agricultural and electric energy generation activities). Revenues originate from both activities and go from the second year onwards, since the first year is unproductive and carries only investment costs.

With regard to the AV system investment cost or capital expenditure (CapEx), the main items are the acquisition and installation of the substructure and mounting structures, PV modules, inverters, pump and the so-called balance-of-system (cables, switchboards, etc.). Appendix B_1 & B_2 includes a breakdown of the cost items involved. With regard to the operating expenditures (OpEx), they can be split in two: First, the annual PV OpEx. Second, the annual costs incurred for crop cultivation beneath AV sheds. Table 3.6 includes estimated crop production costs under the partial shading of an AV shed.

With regard to annual revenues, the main entries are: First, the income from the sale of electricity generated by the PV modules; and second, the income originated from the sale of agricultural produce. With regard to the first, the two variables that intervene are: The annual specific energy yield (kWh/kWp) and the price perceived for the energy generated (Br/kWh). The annual yield will decrease from year 12 onwards, due to the module degradation coefficient above mentioned. Afterwards, we divided the 25-year lifespan into three periods: The first one encompassing the first 9 years, while the second and third period spanning the following eight-year each. Finally, we assigned the OMIP FTS mean price previously calculated, 45.02 Br/MWh, to the first period of 9 years; a price diminished by 5% to the second period (0.95*45.02 = 42.77 Br/MWh); and a price diminished by 10% to the last 8-year period (0.90*45.02 = 40.52 Br/MWh). The reason to assign the foregoing reduced prices to the second and third period is that foreseeably—and unfortunately for generators—increasing solar PV capacity installed in the forthcoming years will lead to decline of wholesale electricity prices (Prol, Steininger, & Zilberman, 2020).

Crop Yield under Full Sunlight is 5,478,709 t/ha (Fischer, Shah, Van Velthuizen, & Nachtergaele, 2001) Total Income under Full Sunlight is 520,190 (EUR/ha) (Tamirat, Abafita, & Tekalegn, 2016)

Table 3.6: Crop production cost under full sunlight and under AV partial shading

Crop Production Cost under Full Sunlight (Br/ha)	**Irrigation Water Saving (%)**	**Crop Production Cost under AV Partial Shading (Br/ha)**
60,651	11.5[(a)]	50,085

[(a)] *Due to scarcity of bibliographic data on water saving for some crops under shade, they are assigned the mean between 14% and 9%*

Revenue Calculation

In all cases, land cost (e.g., rent or purchase) is not considered, because the assumption is that the farm is owned by the regional government.

Table 3.7: Production quantity and selling price of main crop in the suburbs Afar Region [FEWS NET: Ethiopia Price Bulletin, January 31, 2022].

Crops Type	**Total cost (Br/ha)**	**Yield (kg/ha)**	**SalesPrice (Br/kg)**	**Gross income (Br/ha)**	**Net income (Br/ha)**
Wheat	64684	4000	30	120000	55316

The revenue includes electricity sales to the 500 households in the village. This suburb is not yet connected to the grid. As a result, collecting the aforementioned revenue is only a theoretical option at the moment. If the villages are provided with energy and the required local supply infrastructures are established, this revenue may be simply collected. The proposed power selling rate (0.35 Br/kWh) is slightly lower than Ethiopia's current grid energy price (about 0.4 Br/kWh for consumers with yearly demand of 150–300 kWh).

The project's lifespan is 25 years, which is quite long. The nominal annual earnings from the selling of energy has been nearly constant over the years (only affected by a slight decrease in yield, due to degradation rate of solar PV electricity yield caused by solar glass scratches, etc.). NPV is determined by discounting annual net cash flows as an economic signal for the investment.

Table 3.8: Energy Production and Electricity Revenue

Year (N)	**PV Module Degrad. Coeff.**	**Power production (kW)**	**Electricity generation (kwh/kw)**	**Revenues Electricity Sales (PV) (Br)**
0		584,000	1600	52,500

1	1	584,000	1600	52,500
2	1	584,000	1600	52,500
3	1	584,000	1600	52,500
4	1	584,000	1600	52,500
5	1	584,000	1600	52,500
6	1	584,000	1600	52,500
7	1	584,000	1600	52,500
8	1	584,000	1600	52,500
9	1	584,000	1600	52,500
10	1	584,000	1600	52,500
11	0.995	581,080	1592	52,238
12	0.990	575,269	1584	51,975
13	0.985	566,640	1576	51,713
14	0.980	555,307	1568	51,450
15	0.975	541,425	1560	51,188
16	0.970	525,182	1552	50,925
17	0.965	506,801	1544	50,663
18	0.960	486,528	1536	50,400
19	0.955	464,635	1528	50,138
20	0.950	441,403	1520	49,875
21	0.945	417,126	1512	49,613
22	0.940	392,098	1504	49,350
23	0.935	366,612	1496	49,088
24	0.930	340,949	1488	48,825
25	0.925	315,378	1480	48,563
	Total	13,500,433		1,282,316

The levelized cost of energy (LCOE) of a solar PV plant is the ratio between the total costs of the plant (Br) and total electricity production (kWh), both over the economic lifetime of the project, as shown in Equation (3.38). It allows comparison of cost of electricity from different sources.

$$LCOE = \frac{C_{PV}}{\sum_{t=0}^{n} \frac{Et}{(1+r)^t}} \tag{3.38}$$

Where $C_{pv} = \sum_{t=0}^{n} \frac{\text{It} + \text{Mt}}{(1+r)^t}$

Where It = investment expenditures in year t; Mt = operations and maintenance expenditures in year t; Et = electricity generated in year t, d= degradation factor, r = discount rate; n = economic life of the system.

$$C_{pv} = \sum_{t=0}^{25} \frac{20656188.4\ 7}{(1+0.07)^{25}} = 261374798.95 \text{ Br}$$

$$LCOE = \frac{261374\ 79895}{\sum_{t=0}^{n} \frac{584{,}000}{(1+0.7)^{25}}} = 35.37 \text{ Br/MWh}$$

The financial attractiveness of the projects was examined by calculating the financial Net Present Value (NPV) of the investments and the Internal Rate of Return (IRR). These indicators are used to measure the extent to which the project's net revenues are able to repay the investments, regardless of the sources of financing.

The NPV is defined as the sum of the present values of the individual (yearly) cash flaws (Eq. 3.39). A project is financially feasible when the NPV is positive. The higher the NPV, the more profitable the project (Agostini et al., 2016). The NPV is expressed as follows:

$$NPV = -It + \sum_{t=0}^{n} \frac{Rt - Mt}{(1+r)^t} \tag{3.39}$$

Where R = Revenue (Br); Mt= maintenance & operational Costs (Br); NPV= Net present value (Br); r = discount rate; t = economic life of the system.

$$NPV = -20{,}623{,}618.47 + \sum_{t=0}^{25} \frac{8999060 - 32570}{(1+0.07)^t}$$

$$= 92{,}834{,}608.53 \text{ Br}$$

The IRR is defined as the discount rate at which the NPV becomes zero, which means that the present value of future revenues equals the present value of costs (Eq. 3.40). IRR is used to evaluate the future performance of the investment in comparison to other projects of different size, or to a benchmark required rate of return (Agostini et al., 2016). Hence, IRR is defined as:

$$NPV = -It + \sum_{t=0}^{n} \frac{Rt-Mt}{(1+IRR)^t} \tag{3.40}$$

where It = investment expenditures in year t, Rt = revenues year t, Mt = operations and maintenance expenditures in year t; r = discount rate; n = economic life of the system.. If the IRR is higher than the discount rate, the project is viable, otherwise it should be rejected. In general, the higher the IRR, the more desirable it is to undertake the thesis (Agostini et al., 2016).

$$0 = NPV = -20{,}623{,}618.47 + \sum_{t=0}^{25} \frac{8999060-32570}{(1+IRR)^t}$$

IRR = 11.416%

CHAPTER FOUR

Results and Discussions

4.1 System sizing results

AV system is the combination between solar photovoltaic power generation and plant cultivation. The land equivalent ratio (LER) is a well-established statistic for evaluating the success of dual-land use systems like agroforestry (Seserman, 2018) and thereby AV. The LER only accounts for system income, not expenditures. The levelized cost of electricity (LCoE), on the other hand, is a benchmark for energy generation systems that calculates cost relative to power yield but ignores agricultural producing activity. The internal rate of return (IRR) was used as the criterion for determining profitability in this case. Once the income and expenditure from both agricultural and energy producing activities were accounted for, the IRR could be calculated easily.

A 153 kWp ground-mounted solar panel system was designed and constructed. After that, a plant plot sizing 1 x 7 m under this solar panel was design as well as 150 vegetation of wheat crop is grown. The potential of AV system consisting of efficiency of solar power generation, the wheat yield and the land equivalent ratio of system were monitored and evaluated. In addition, 1,600 kg of wheat yield was obtained. The total value of both systems could make up to 656.34Br a month ($3.27 and $7.64 from solar power generation and plant production, respectively). The land equivalent ratio (LER) of system was 1 .80 which was indicated that the AV system could increase the land value up to 80%.

The modeled pumping system includes a vertical stainless steel multistage centrifugal pump coupled with a three-phase 92 kW, 50 Hz, 380 V AC nominal voltage, 2 poles and 2870 RPM nominal speed squirrel cage induction motor. The modeled pressure sensor is a 25 Bar ranged pressure switch in constant speed control strategy and an analog piezoelectric pressure transmitter with 24 V DC feed voltage and 4-20 mA output current in variable speed control strategy. The applied nominal voltage is 50 Hz, 380 V AC for both strategies. The star-delta is a three-phase 92 kW converter for the electrical pump.

The LCOE computed value is 35.37 Br/kWh (with the energy yield discounted to its present value at a baseline discount rate of 7%). The electricity selling tariff is the most crucial characteristic on the revenue side. As a result, its impact on NPV is computed, and the findings are shown in details. The NPV will begin to decline if the selling tariff falls below 8.7 Br/kWh. As a result, this is the selling tariff that breaks even.

Given the assumptions made with respect to revenues and expenses, an investment in an AV-system seems to be profitable. This is indicated by a positive NPV of 52,993,501.63 Br per ha. The NPV of the project splits up in a surplus of 42,993501.63 contributed by agriculture and around 10,000,000 on the part of PV. Profitability of agriculture is about 81.13% under this production. These efficiency gains mainly result from lower variable cost at almost stable yield and earnings. Indeed, there are also gains with respect to PV: Keeping other variables constant, the elimination of land cost reduces OPEX by about 12% alleviating total losses by almost 30%. Profitability of PV is about 20% higher than under mono production Moreover, all these benefits are large enough to balance out the fierce rise in CAPEX. Fig. 4.1 gives a graphical overview of most relevant cost items. The first pie chart shows the structure of agricultural costs within the AV-system whereas the second one depicts this structure for PV-related costs.

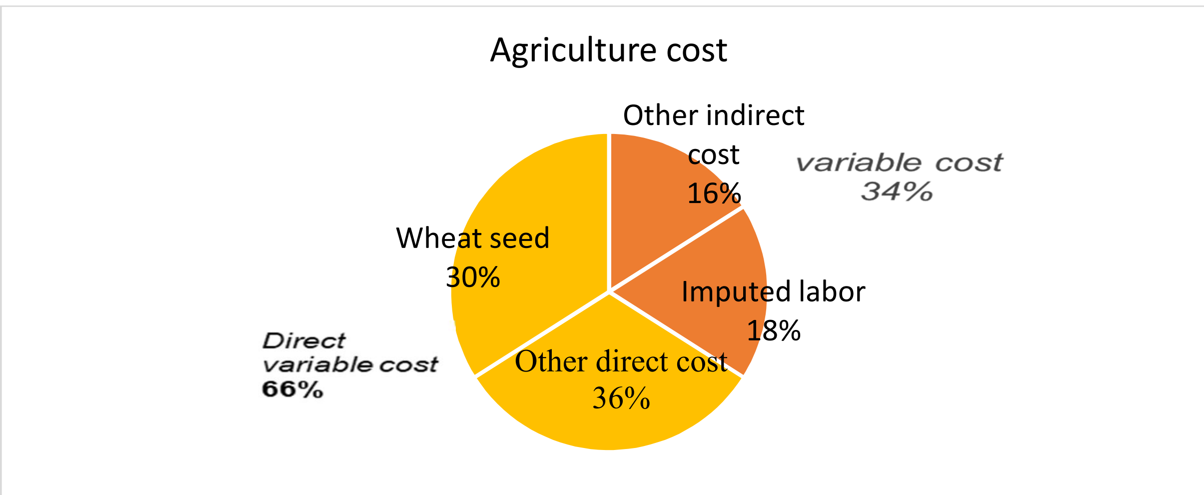

Figure 4.1a: Cost structure of agriculture as part of AV production

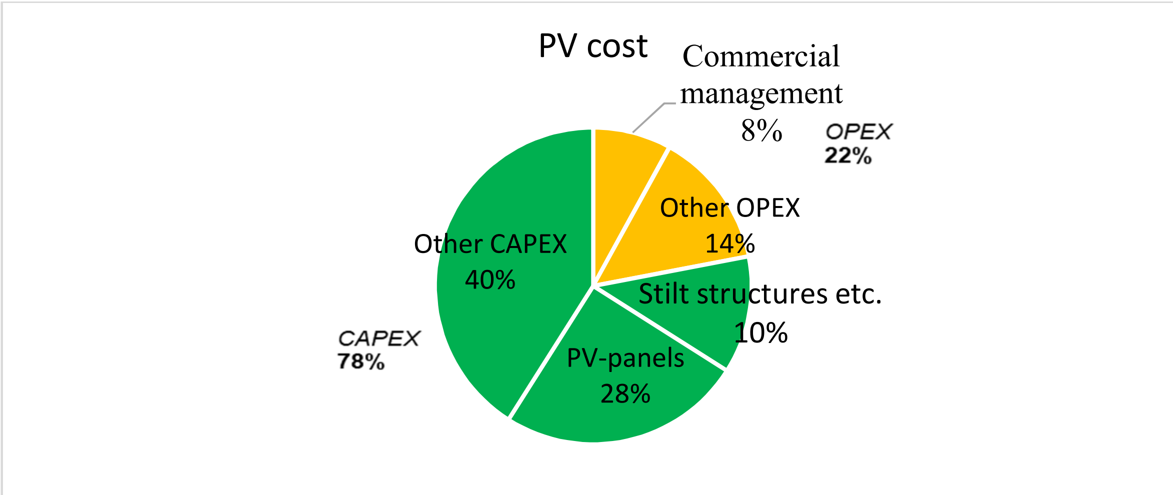

Figure 4.1b: Cost structure of PV as part of AV production

With respect to scope and added economic value, total sales of around 9.6 million birr per ha split up in 9 million birr from agriculture and 0.6 million birr from PV. This means, sales from agriculture are about 15 times more worth than those from PV (considering the whole 80 ha). This relation is also prevalent in terms of cost. Fig. 4.1c illustrates this by the structure of AV cost incorporating agricultural and PV cost of Fig. 4.1a and Fig. 4.1b.

Considering potential learn effects related to high elevation of PV-panels, it might be interesting to know the maximum rise of expenses on mounting structures etc. to still attain an equal NPV as expected by the mono PV project.

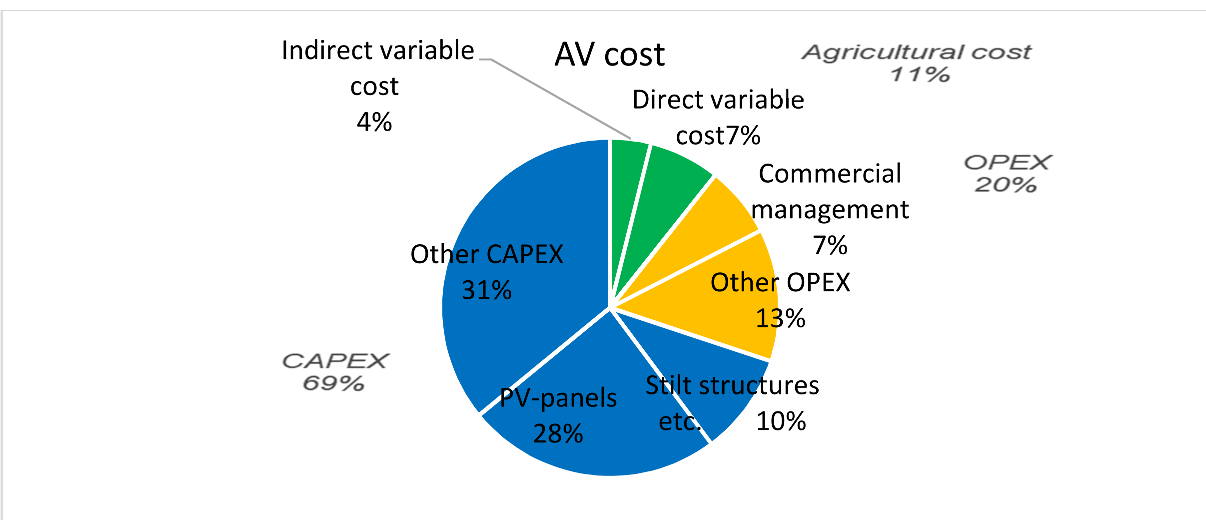

Figure 4.1c: Cost structures of AV production

4.2 Cost Analysis of the Proposed System using HOMER

As the load of the motor was associated with a water tank storage, so a deferrable load was used in HOMER and as the motor is running for 8 hours, so 92 x 8 = 736 kWh is the storage capacity required. The overall proposed system in HOMER appears as shown in figure 4.2. The PV panel used was Generic flat plat plate PV to design a PV panel network.

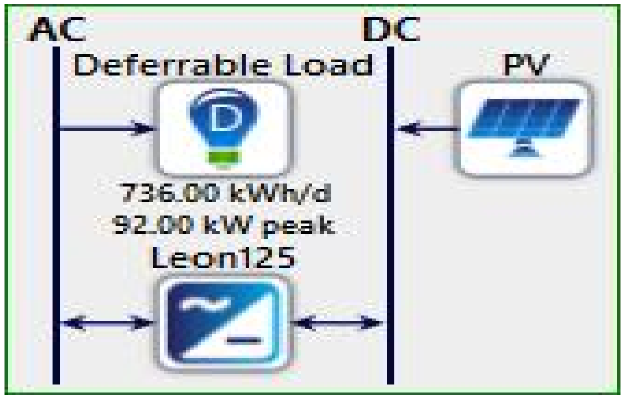

Figure 4.2: Proposed AV system

After the simulation of the overall proposed AV system was performed. The PV Panel network requirement came out to be 140 kW and the inverter requirement came out to be 125 kW, which was fulfilled by a 125 kW Leonics GTP-507. The overall result is shown in the figure 4.3.

The overall cost summary for the proposed system was performed in HOMER, as shown in figure 4.3. The total net present cost of the proposed system came out to be 23,804,737.46Br, levelized cost of energy was 15.37Br and the operating cost of the proposed system was calculated by HOMER is 434,055.20Br per year.

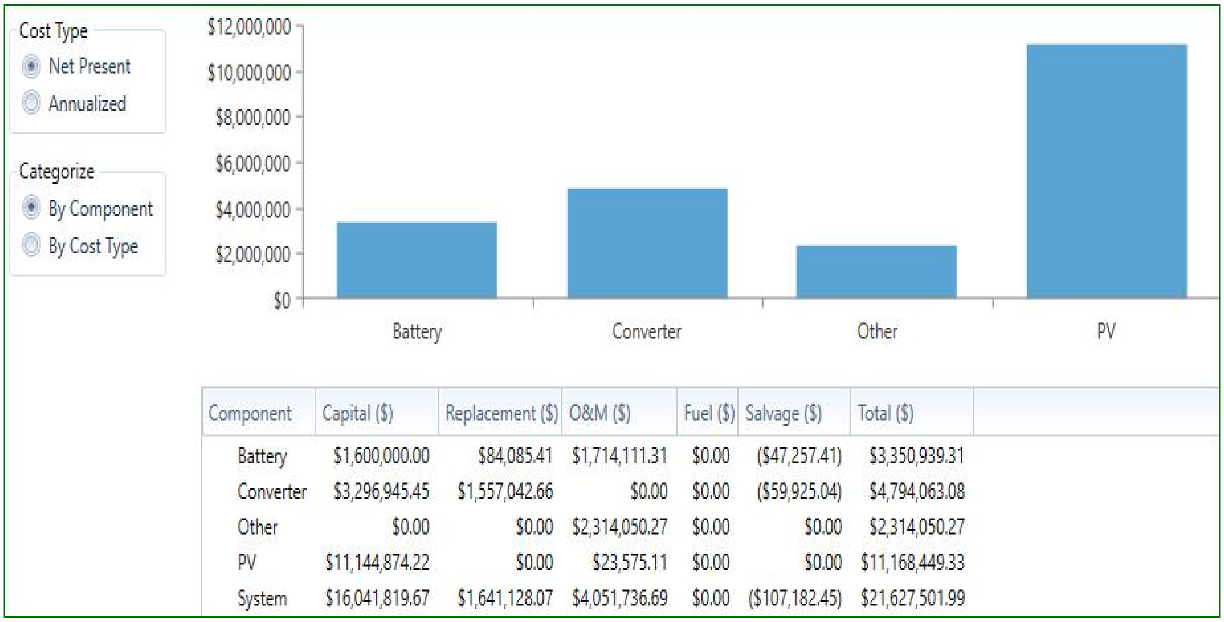

Component	Capital ($)	Replacement ($)	O&M ($)	Fuel ($)	Salvage ($)	Total ($)
Battery	$1,600,000.00	$84,085.41	$1,714,111.31	$0.00	($47,257.41)	$3,350,939.31
Converter	$3,296,945.45	$1,557,042.66	$0.00	$0.00	($59,925.04)	$4,794,063.08
Other	$0.00	$0.00	$2,314,050.27	$0.00	$0.00	$2,314,050.27
PV	$11,144,874.22	$0.00	$23,575.11	$0.00	$0.00	$11,168,449.33
System	$16,041,819.67	$1,641,128.07	$4,051,736.69	$0.00	($107,182.45)	$21,627,501.99

Figure 4.3: Simulation details for the proposed system in HOMER software

The proposed system cash flow over the 25 years lifetime can be seen in figure 4.4. It can be seen that an initial investment of $16,041,819.67 is required and, then an annual investment of $4,520.83 is required to keep the system running. A further injection of $3,296,945.45 in the 13th year of the 25 years project life is required. After 25 years of the project's life cycle, the system would have a salvage value of $107,182.45.

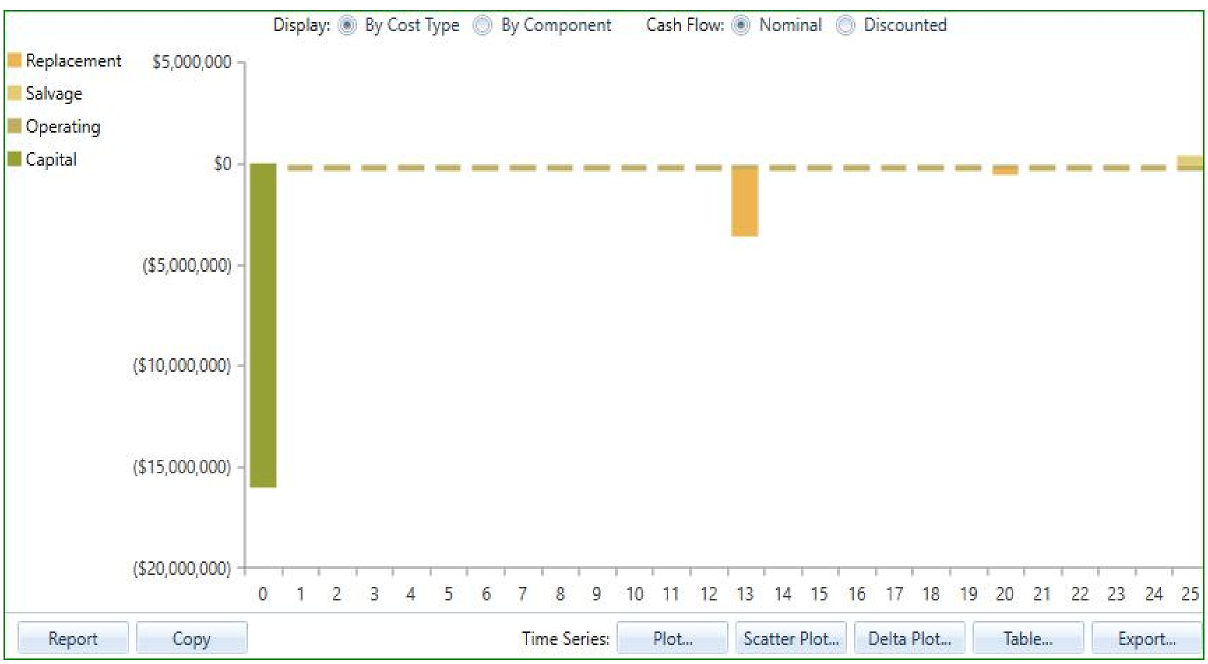

Figure 4.4: Cash Flow for the proposed system

Costing of the Water Tank

Local rate for construction including material, labour, digging and supervision lumped together costs ETB 100/m^2.

As the tank is closed from top, so the total surface area can be calculated using Equation (4.1).

$$\text{Surface Area} = 2\pi r^2 + 2\pi r h \quad (4.1)$$

Surface area = $2 \times 3.14 \times 11.285^2 + 2 \times 3.142 \times 11.285 \times 6$

Surface area = 1225.6 m^2

Overall price for tank is 1225.6 × 300 = ETB 367,681

4.3 PVSyst Result for the proposed system

The system was also sized using PVSyst software to analyze the system's performance with tank storage. In developing the system, the program assisted us in selecting the proper pump, along with the PV panels and inverters. Several data set were used, such as total pump head, water demand, pump level, and information about the site's features. It aided us in determining the proper diameter and length of the pipe, as well as the tank's features. The benefit of using the Pvsyst program is that it assisted us in sizing the storage tank capable of keeping water when up to one days of autonomy are taken into account, which is not achievable with the Homer software.

The irrigation power requirements were determined to be 92 kW. To achieve a system power of 153.6 kW, a 98.4% inverter was proposed. For the sizing, solar panels (384 panels) with a capacity of 400 watts were selected. The panels were set up in a 16 parallel, 24 series layout.

The simulation included input variables such as weather data, water demand, and pumping head. The simulation results are depicted in the figures below.

PVSYST V6.81		03/07/22	Page 1/5

Pumping PV System: Basic simulation parameters

Project :	**New Project**			
Geographical Site	**Aysit**		Country	**Ethiopia**
Situation	Latitude	14.24° N	Longitude	40.29° E
Time defined as	Legal Time	Time zone UT+3	Altitude	-130 m
	Albedo	0.20		
Meteo data:	**Aysit**	Meteonorm 7.2, Sat=100% - Synthetic		
Simulation variant :	**New simulation variant**			
	Simulation date	03/07/22 16h07		

Simulation parameters

Pumping System parameter	System type	**Deep Well to Storage**		
Well characteristics	Static level depth	16.0 m	Specific drawdown	0.00 m / m³/h
(Diameter 15 cm)	Pump depth	30.0 m	Max. pumping depth	27.5 m
Storage tank	Volume	2400.0 m³	Diameter	22.9 m
Feeding by top	Feeding altitude	5.7 m	Height (full level)	5.8 m
Hydraulic circuit	Piping length	70 m	Pipes PE50	Dint = 191 mm
	Number of elbows	3		
Water needs	Yearly constant:	2400.00 m³/day		
Pump	Model	**SP 160-8**		
	Manufacturer	Grundfos		
Pump Technology	Centrifugal Multistage	Deep well pump	Motor	Async. AC motor, tripha

Operating conditions	**head Min**	**head Nom**	**head Max**	
	20.0	80.0	170.0	mWater
Corresponding maximum Flow Rate	362.85	238.33	59.37	m³
Required power	93000	90000	87000	W

Collector Plane Orientation	Tilt	14°	Azimuth	0°
PV Array Characteristics				
PV module Si-mono	Model	**TD672M-400-L**		
Original PVsyst database	Manufacturer	Talesun Solar (suzhou)		
Number of PV modules	In series	24 modules	In parallel	16 strings
Total number of PV modules	Nb. modules	384	Unit Nom. Power	400 Wp
Array global power	Nominal (STC)	**154 kWp**	At operating cond.	139 kWp (50°C)
Array operating characteristics (50°C)	U mpp	871 V	I mpp	159 A
Total area	Module area	**768 m²**	Cell area	697 m²
Control device	Model	Generic device (optimised for the system)		
	System Configuration	**Fixed V DC-AC inverter**		

Figure 4.5: PVSyst Simulation Results with basic simulation parameters

4.4 MATLAB/SIMULINK Simulation Result Analysis of the proposed System

MATLAB/Simulink was used to run the simulations in this investigation since it can handle exceedingly complex simulations (Fara & Craciunescu, 2017). A PV system and an appropriate power supply were used to imitate the induction motor. Finally, the system and pump calculations were validated by testing the pump and induction motor models, as well as the auxiliary components and pipes.

The output voltage of the PV array is 48 V. In the system, a buck converter is used to decrease the voltage level from 1000V to 380V to run the induction motor to lift groundwater. A three-level bridge converter is used as an inverter to convert the DC component into AC component. This system consists of a large water tank, which can store around 2400 m^3 of water.

The PV voltage and PV current of solar PV array at $G=1000W/m^2$ and $T=25\ ^0C$ are shown in Figure.4.5. V_PV the steady state value is around 1000 V, which is expected and I_PV represent the PV current with a value of 153A.

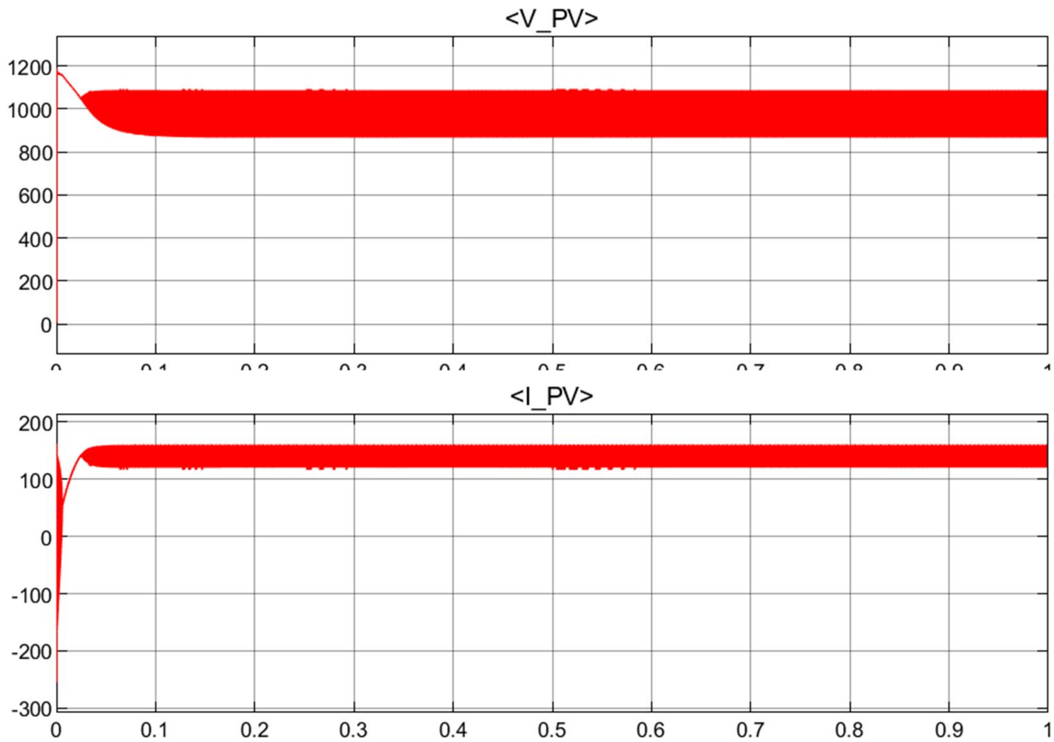

Figure 4.5: PV voltage and current

The buck converter plays an important role in the reduction of the PV voltage from 1000V to 380V, which is the voltage required by the motor pump. V_dc denotes the bucked-down dc voltage in Figure.4.6.

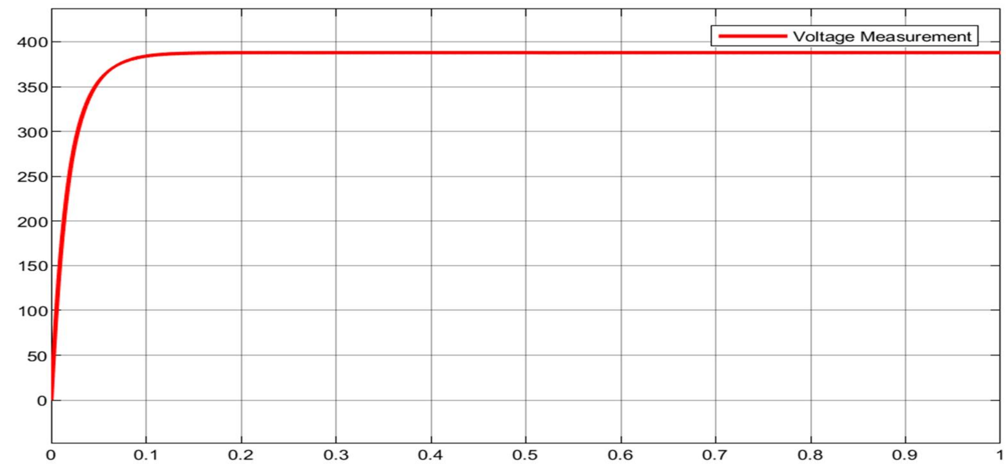

Figure 4.6: Buck converter output voltage

Then the inverter converts this DC unit into AC unit to run the motor. I_ac and V_ac indicate the converted ac current and voltage accordingly. The following figure shows that line voltage is 380V which match the expectation.

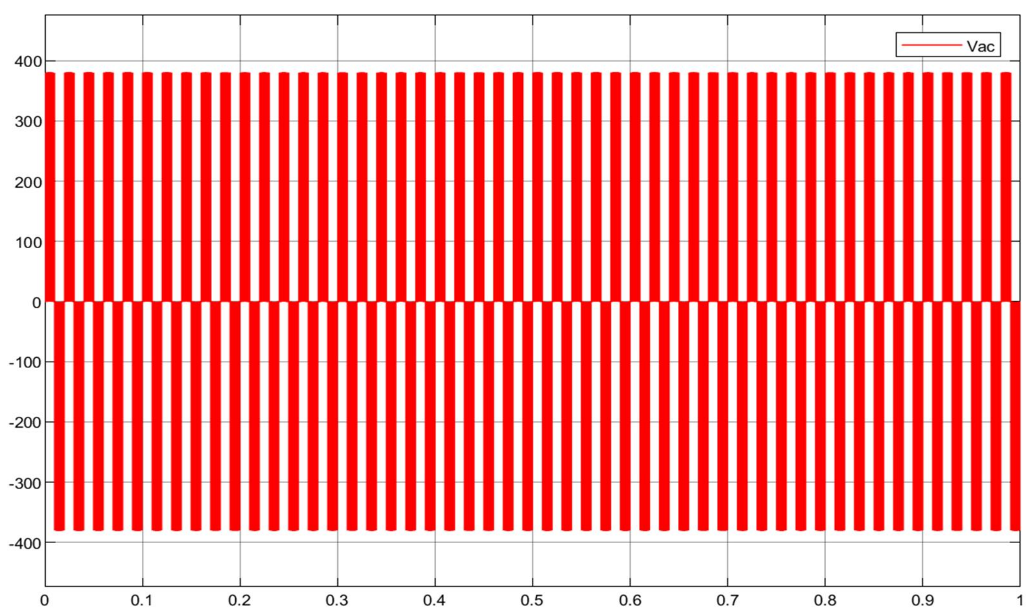

Figure 4.7: Inverter Output voltage

The induction motor rotor speed is 2870 rpm, in the system shown in Figure.4.8. After one second the rotor speed decreases sharply because the atmospheric condition is changing rapidly.

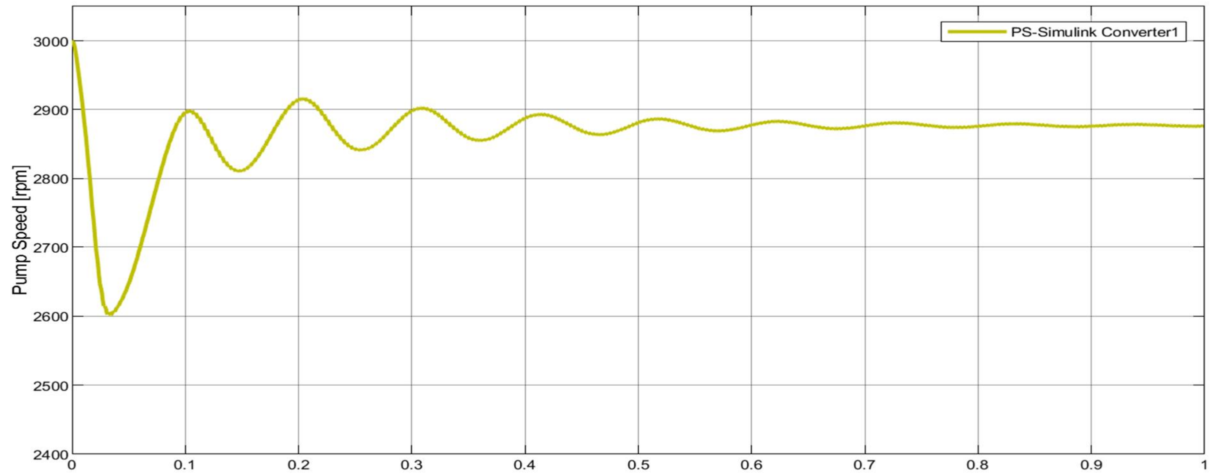

Figure 4.8: Rotor speed of the proposed system

The water discharge (m^3/s) is demonstrated in Figure.4.9. Water discharge is 0.095 m^3/s or 342 m^3/h, which then decreases to $7 \times 10{-}3$ [m3/sec] which is slightly lower than the actual calculated value. After eight hours of operation, the tank water level would reach at least 5.86 m and volume of lifted water per day would be 2360 m^3.

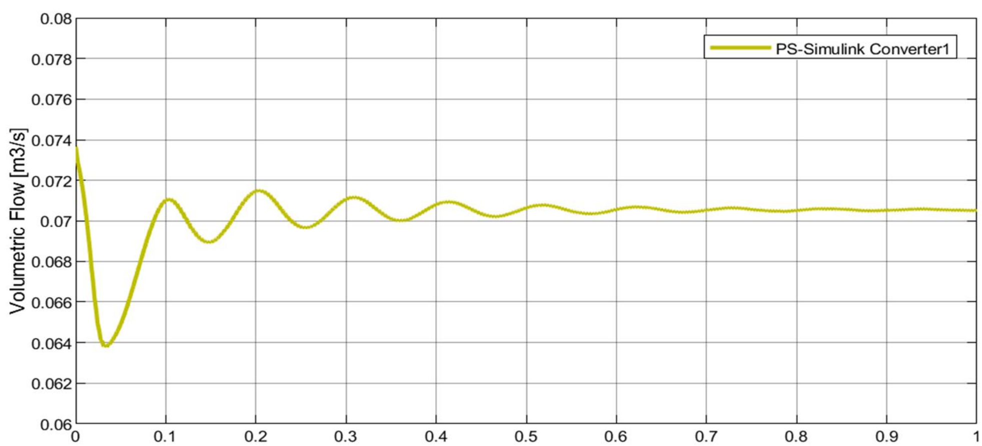

Figure 4.9: Water discharge and tank water level of the proposed system

Figure 4.10 shows the shaft power of the pump [kW] against time [sec]. The shaft power of the pump gives the same results as the motor speed, as shown in the figure. The total power of the shaft is 92 kW.

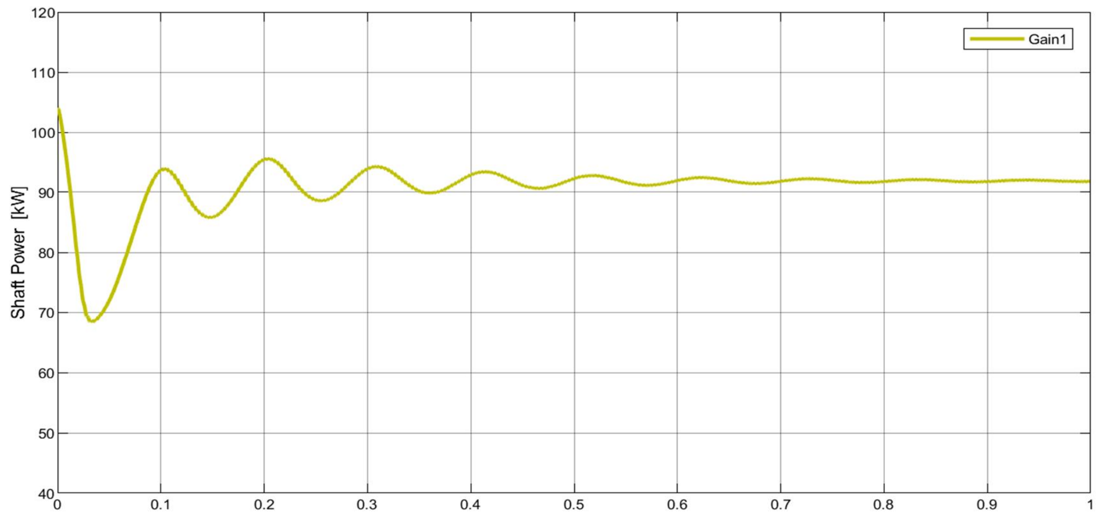

Figure 4.10: Pump output power

Discussion

Arid-zone of the Afar regional State, Dallol is among the best positioned because of the abundance of sunlight for supporting renewable energy through PV, but projections of increasing ambient temperatures suppressed this renewable energy source potential because of PV panel sensitivity to increases in temperature. While PV panels vary, their temperature coefficient—the rate of performance decline for every 1 °C increase in temperature >25 °C—illustrates that PV panel efficiency decreases by an average of ~0.6% ºC–1). Within natural ecosystems, vegetation reduces heat gain and storage in soils by creating surface shading, though the degree of shading varies among plant types. Transitions of liquid water-to-water vapour loss to the atmosphere through evapotranspiration—the combined water loss from soils (evaporation) and vegetation (transpiration)—use energy absorbed by vegetation and surface soils. Because PV installation have gravel as groundcover, with little to no vegetation, they have little to no means of energy dissipation through latent heat exchange and thus are subjected to more sensible heat.

The ground-mounted Solar power generation that combine with agriculture could generate electricity similar to or more than a solar power system that is not co-produced with agriculture because such a power system is designed for the purpose of generating electricity. The crop cultivation under the photovoltaic panels may result in lower panel temperatures. The voltage increases and there are results in more electricity.

We suggest that this energy- and food-generating ecosystem may become an important—but as yet quantitatively uninvestigated—mechanism for maximizing crop yields, efficiently delivering water to plants and generating renewable energy in dryland environments. We demonstrate proof of concept for AV as a food–energy– water system approach in drylands by simultaneously monitoring the physical and biological dimensions of the novel ecosystem. We hypothesized that colocating solar and agricultural could yield several significant benefits to multiple ecosystem services, including

(1) Water Conservation in Irrigation: maximizing the efficiency of water used for plant irrigation by decreasing evaporation from soil and transpiration from crop canopies.

(2) Farm Yield Improvement: preventing depression in photosynthesis due to heat and light stress thus allowing for greater carbon uptake for growth and reproduction and

(3) Rural Electrification: transpirational cooling from the understorey crops lowering temperatures on the underside of the panels, which could improve PV efficiency.

We focused on common agricultural species that represent different adaptive niches for dryland environments: cherry wheat (*Triticum aestivum*). We created an AV system by planting these species under a PV array—2.5 m off the ground at the lowest end and at a tilt of 14°—to capture the physical and biological impacts of this approach. Throughout the average three-month summer growing season we monitored incoming light levels, air temperature and relative humidity continuously using sensors mounted 2 m above the soil surface, and soil surface temperature and moisture at 5-cm depth.

Our work is to explored the feasibility of PV irrigation systems with enough power to supply water to professional agricultural exploitations (big farmers and irrigator communities) in the range of tens and hundred kW.

CHAPTER FIVE

Conclusions and Recommendations

5.1 Conclusion

We take an integrative approach—monitoring microclimatic conditions, PV panel temperature, soil moisture and irrigation water use, plant ecophysiological function and plant biomass production within this AV ecosystem and in traditional PV installations and agricultural settings to quantify trade-offs. we discover that shading by the PV panels provides multiple additive and synergistic benefits, including reduced plant drought stress, greater food production and reduced PV panel heat stress. The results presented here provide a foundation and motivation for future explorations towards the resilience of food and energy systems under the long run projected increased environmental stress involving heat and drought. Partial shade under the solar modules increased the farm's crop yields and high levels of solar radiation increased solar power production. The land use efficiency for wheats increased by 86 percent.

For this thesis, a detailed design and cost analysis for an agrivoltaic system was performed in HOMER software. The system requirements came out to be 140 kW for the PV panel network and the inverter rating came out to be 125 kW. The net present cost for the overall system came out to be 26,804,737.46Br, the levelized cost of energy came out to be 50.46Br and the operating cost for the system came out to be 80,257.65Br. Then, for the designed system, a detailed dynamic analysis was conducted in MATLAB/Simulink, which validated the HOMER software results. Based on the economical analysis results for agrivoltaic systems, it was concluded that the proposed system was a more feasible solution for Afar region conditions.

5.2 Recommendations

On the effectiveness of AV systems in creating potent synergies between agricultural and solar energy, it is impossible to draw a firm conclusion. In fact, the models utilized demonstrate that the presence of solar panels allows for the reduction of irrigation and offers crops protection from climate change for a number of crops. However, not all crops have been examined for the use of AV. Only wheat is the subject of this thesis.

The real work is not done yet and recommended to put the theoretical work to the real environment since this system have further advantages The installation of AV systems must be expanded in the future to include further plants. There is a general lack of knowledge regarding AV among farmers. Maintaining and running a solar power plant takes specific knowledge and training, just like any other occupation.

References

Abu-Aligah, M. (2011). Design of Photovoltaic Water Pumping System and Compare it with Diesel Powered Pump. *Jordan Journal of Mechanical & Industrial Engineering*, *5*(3).

Adeh, E. H., Good, S. P., Calaf, M., & Higgins, C. W. (2019). Solar PV power potential is greatest over croplands. *Scientific Reports*, *9*(1), 1–6.

Agostini, A., Battini, F., Padella, M., Giuntoli, J., Baxter, D., Marelli, L., & Amaducci, S. (2016). Economics of GHG emissions mitigation via biogas production from Sorghum, maize and dairy farm manure digestion in the Po valley. *Biomass and Bioenergy*, *89*, 58–66.

Alkarrami, F., Iqbal, T., Pope, K., & Rideout, G. (2020). *Dynamic Modelling of Submersible Pump Based Solar Water-Pumping System with Three-Phase Induction Motor Using MATLAB*. 20–64. https://doi.org/10.4236/jpee.2020.82002

Anis, W. R., & Nour, M. A. (1994). Optimum design of a photovoltaic powered pumping system. *Energy Conversion and Management*, *35*(12), 1123–1130.

Arab, A. H., Chenlo, F., & Benghanem, M. (2004). Loss-of-load probability of photovoltaic water pumping systems. *Solar Energy*, *76*(6), 713–723.

Arrouf, M., & Ghabrour, S. (2007). Modelling and simulation of a pumping system fed by photovoltaic generator within the Matlab/Simulink programming environment. *Desalination*, *209*(1–3), 23–30.

Artru, S., Garré, S., Dupraz, C., Hiel, M.-P., Blitz-Frayret, C., & Lassois, L. (2017). Impact of spatio-temporal shade dynamics on wheat growth and yield, perspectives for temperate agroforestry. *European Journal of Agronomy*, *82*, 60–70.

Barron-Gafford, G. A. (2016). *Agrivoltaics in drylands: Co-location has food, water, and renewable energy benefits*.

Bhende, C. N., Mishra, S., & Malla, S. G. (2011). Permanent magnet synchronous generator-based standalone wind energy supply system. *IEEE Transactions on Sustainable Energy*, *2*(4), 361–373.

Bogale, B., & Alemayehu, A. (2012). Optimal Design of a Standalone Photovoltaic Power Supply System for Air Conditioning Application at Samara University as an Alternative to Diesel Generator Source. *Science, Technology and Arts Research Journal*, *1*(2), 65–71.

Burleigh, J. R., Allan, R. E., & Vogel, O. A. (1965). Varietal Differences in Seedling Emergence of Winter Wheats as Influenced by Temperature and Depth of Plants 1. *Agronomy Journal*, *57*(2), 195–198.

Coşgun, A. E. (2021). The potential of Agrivoltaic systems in TURKEY. *Energy Reports*, *7*, 105–111.

Dinesh, H., & Pearce, J. M. (2016). The potential of agrivoltaic systems. *Renewable and Sustainable Energy Reviews*, *54*, 299–308.

Dorling, D. (2021). World population prospects at the UN: our numbers are not our problem? In *The Struggle for Social Sustainability* (pp. 129–154). Policy Press.

Dupraz, C., Marrou, H., Talbot, G., Dufour, L., Nogier, A., & Ferard, Y. (2011). Combining solar photovoltaic panels and food crops for optimising land use: Towards new agrivoltaic schemes. *Renewable Energy*, *36*(10), 2725–2732.

Elamri, Y., Cheviron, B., Lopez, J., Dejean, C., & Belaud, G. (2018). Water budget and crop modelling for agrivoltaic systems : Application to irrigated lettuces. *Agricultural Water Management*, *208*(July), 440–453. https://doi.org/10.1016/j.agwat.2018.07.001

Fara, L., & Craciunescu, D. (2017). Output Analysis of Stand-alone PV Systems: Modeling, Simulation and Control. *Energy Procedia*, *112*, 595–605. https://doi.org/https://doi.org/10.1016/j.egypro.2017.03.1125

Fischer, G., Shah, M. M., Van Velthuizen, H. T., & Nachtergaele, F. O. (2001). *Global agro-ecological assessment for agriculture in the 21st century*.

Fudholi, A., Sopian, K., Yazdi, M. H., Ruslan, M. H., Ibrahim, A., & Kazem, H. A. (2014). Performance analysis of photovoltaic thermal (PVT) water collectors. *Energy Conversion and Management*, *78*, 641–651.

Glasnovic, Z., & Margeta, J. (2007). A model for optimal sizing of photovoltaic irrigation water pumping systems. *Solar Energy*, *81*(7), 904–916.

Goetzberger, A, & Zastrow, A. (2015). *On the Coexistence of Solar-Energy Conversion and Plant Cultivation On the Coexistence of Solar- Energy Conversion and Plant Cultivation*. *5919*(November). https://doi.org/10.1080/01425918208909875

Goetzberger, Adolf, & Zastrow, A. (1982). On the coexistence of solar-energy conversion and plant cultivation. *International Journal of Solar Energy*, *1*(1), 55–69.

Harishankar, S., Kumar, R. S., Sudharsan, K. P., Vignesh, U., & Viveknath, T. (2014). Solar powered smart irrigation system. *Advance in Electronic and Electric Engineering*, *4*(4), 341–346.

Hsu, D. D., O'Donoughue, P., Fthenakis, V., Heath, G. A., Kim, H. C., Sawyer, P., … Turney, D. E. (2012). Life cycle greenhouse gas emissions of crystalline silicon photovoltaic electricity generation: systematic review and harmonization. *Journal of Industrial Ecology*, *16*, S122–S135.

Hussein, A. K. (2016). Applications of nanotechnology to improve the performance of solar collectors – Recent advances and overview. *Renewable and Sustainable Energy Reviews*, *62*, 767–792. https://doi.org/10.1016/j.rser.2016.04.050

Jia, S.-F., Li, C.-F., Dong, S.-T., & Zhang, J.-W. (2011). Effects of shading at different stages after anthesis on maize grain weight and quality at cytology level. *Agricultural Sciences in China*, *10*(1), 58–69.

Li, X., Cai, J., Li, H., Bo, Y., Liu, F., Jiang, D., … Cao, W. (2012). Effect of shading from jointing to maturity on high molecular weight glutenin subunit accumulation and glutenin macropolymer concentration in grain of winter wheat. *Journal of Agronomy and Crop Science*, *198*(1), 68–79.

Majumdar, D., & Pasqualetti, M. J. (2018). Dual use of agricultural land: Introducing 'agrivoltaics' in Phoenix Metropolitan Statistical Area, USA. *Landscape and Urban Planning*, *170*, 150–168.

Malu, P. R., Sharma, U. S., & Pearce, J. M. (2017). Agrivoltaic potential on grape farms in India. *Sustainable Energy Technologies and Assessments*, *23*, 104–110.

Marrou, H., Dufour, L., & Wery, J. (2013). How does a shelter of solar panels influence water flows in a soil–crop system? *European Journal of Agronomy*, *50*, 38–51. https://doi.org/https://doi.org/10.1016/j.eja.2013.05.004

Mavani, D. D., Chauhan, P. M., & Joshi, V. (2019). Beauty of Agrivoltaic System regarding double utilization of same piece of land for Generation of Electricity & Food Production. *Int. J. Sci. Eng. Res*, *10*(6).

Oudes, D., & Stremke, S. (2021). Next generation solar power plants? A comparative analysis of frontrunner solar landscapes in Europe. *Renewable and Sustainable Energy Reviews*, *145*, 111101.

Pande, P. C., Singh, A. K., Ansari, S., Vyas, S. K., & Dave, B. K. (2003). Design development and testing of a solar PV pump based drip system for orchards. *Renewable Energy*, *28*(3), 385–396.

Pearman, I., Thomas, S. M., & Thorne, G. N. (1978). Effect of nitrogen fertilizer on growth and yield of semi-dwarf and tall varieties of winter wheat. *The Journal of Agricultural Science*, *91*(1), 31–45.

Proctor, K. W., Murthy, G. S., & Higgins, C. W. (2020). *Agrivoltaics Align with Green New Deal Goals While Supporting Investment in the US'Rural Economy. Sustainability 2021, 13, 137*. s Note: MDPI stays neu-tral with regard to jurisdictional claims in ….

Prol, J. L., Steininger, K. W., & Zilberman, D. (2020). The cannibalization effect of wind and solar in the California wholesale electricity market. *Energy Economics*, *85*, 104552.

Ravi, S., Macknick, J., Lobell, D., Field, C., Ganesan, K., Jain, R., … Stoltenberg, B. (2016). Colocation opportunities for large solar infrastructures and agriculture in drylands. *Applied Energy*, *165*, 383–392.

Schindele, S., Trommsdorff, M., Schlaak, A., Obergfell, T., Bopp, G., Reise, C., … Weber, E. (2020). Implementation of agrophotovoltaics : Techno-economic analysis of the price-performance ratio and its policy implications. *Applied Energy*, *265*(March), 114737. https://doi.org/10.1016/j.apenergy.2020.114737

Sekiyama, T., & Nagashima, A. (2019). Solar sharing for both food and clean energy production: performance of agrivoltaic systems for corn, a typical shade-intolerant crop. *Environments*, *6*(6), 65.

Senol, R. (2012). An analysis of solar energy and irrigation systems in Turkey. *Energy Policy*, *47*, 478–486.

Seserman, D.-M. (2018). Benefits of agroforestry systems for land equivalent ratio-case studies in Brandenburg and Lower Saxony, Germany. *European Agroforestry Conference-Agroforestry as Sustainable Land Use, 4th*. EURAF.

Simonneau, T., Sourd, F., Pechier, P., Hamard, P., Frisson, T., Ryckewaert, M., & Christophe, A. (2017). Increasing the total productivity of a land by combining mobile photovoltaic panels and food crops. *Applied Energy*, *206*, 1495–1507.

Skidmore, E. L., & Siddoway, F. H. (1978). Crop residue requirements to control wind erosion. *Crop Residue Management Systems*, *31*, 17–33.

Tamirat, N., Abafita, J., & Tekalegn, E. (2016). Adoption and Impact of Row Planting of

Wheat Crop on Household Livelihood:-A Case Study of Duna Woreda in Hadiya Zone, Ethiopia. *Ethiopian Economics and Ethiopian Strategy S (ESSP) Of*, *19*.

Trommsdorff, M. (2019). *An Economic Analysis of Agrophotovoltaics : Opportunities , Risks and Strategies towards a More Efficient Land Use * Maximillian Trommsdorff ***. (December).

Weselek, A. (2019). *Agrophotovoltaic systems : applications , challenges , and opportunities . A review*.

Weselek, A., Ehmann, A., Zikeli, S., Lewandowski, I., Schindele, S., & Högy, P. (2019). Agrophotovoltaic systems: applications, challenges, and opportunities. A review. *Agronomy for Sustainable Development*, *39*(4), 1–20.

Wolde-Ghiorgis, W. (2002). Renewable energy for rural development in Ethiopia: the case for new energy policies and institutional reform. *Energy Policy*, *30*(11–12), 1095–1105.

Appendices

Appendix A: Head calculation

Parameter/Project	**Sheder**
I) Given Parameters	
Coordinates	14N,40.12E
Borhole elevation (m)	677
Tank elevation above borehole head (m)	6
Borhole depth (m)	30
Casing Diameter (mm)	203.2
Casing type	Pvc
Safe yeild(L/s)	1.6
SWL(M)	16.05
DWL(M)	26.8
Pump position @ safe yield (m)	**27.5**
Type of riser pipe	GI
Size of riser (mm)	50
Desired discharge (m^3/day)	**2400**
Length of pipe line(m) from borehole head to tank	700
Type of pipe (Bore Hole to reservoir)	HDPE
Size of pipe (mm) (Borehole to reservoir)	200
II) Calculated Parameters	
Hazen Wiliam cofficient for GI pipe	120
Hazen Wiliam cofficient for HDPE pipe	140
Safe yeild [m3/hr]	5.8
Desired discharge (m3/hr, assuming 7hr sun shine)	342.85
Static Head	**48.8**

Static Head - DWL to Borehole Surface [m]	26.8
Static Head - Borehole Surface to Reservoir [m]	22
Dynamic Head	**32**
Dynamic Head - GI Riser Pipe [m]	5
Dynamic Head - Transmition Line [m]	27
Residual Pressure	9
Total Head of pump (T. Dynamic + T. Static) [m]	**80.5**
Minimum PN rating of riser Pipe [Bar]	**6.08**
Minimum PN rating of transmission Pipe [Bar]	**2.5**

Appendix B: Cost Values for AV system

Appendix B₁: AV system initial investment cost or capital expenditure, CapEx

Item No.	DESCRIPTION	Unit	Qty	UNIT PRICE (Br)	TOTAL PRICE (Br)
I	**Supply , installation, Testing and Commissioning work as the design, Bill of quantities and drawing for the following:-**				
1.1	Solar Panel 400 W Mono Crystalline	Pcs	384	12,154.91	4,667,485.44
1.2	PV Combiner Box, 6 Stringer, 15 A Input, 100 A Output	Pcs	4	181,332.00	725,328.00
1.3	Main Combiner Box, 4 Stringer, 120 A Input, 600 A Output	Pcs	1	589,329.00	589,329.00
1.4	AC Power Pack 132 Kw	Pcs	1	1,325,990.25	1,325,990.25
1.5	Solar Pump Inverter 132 Kw	Pcs	1	2,175,984.00	2,175,984.00
1.6	Water Level Sensor with 150 Mtr cable	SET	1	184,165.31	184,165.31

1.7	AC Filter (Outlet Filter) 132 Kw	Pcs	1	662,995.13	662,995.13
1.8	Flexible rubber cable, 3 core 95mm Pure Copper	m	150	4,051.64	607,745.53
1.9	Solar PV cable 6 mm	Roll	32	11,049.92	353,597.40
1.10	Submersible Water Pump with Motor and cooling sleeve, 92 Kw, 400Vx3 phase, 6 inch pump outlet (Q=50l/s ,H=106m and Casing diameter=12")	Pcs	1	3,059,977.50	3,059,977.50
1.11	than 25 years, with standing: Min. Wind speed: 45 m/s, 3s gust Height Above Ground (Ground Clearance) 750 mm configuration 6×16 Land scape Foundation : Concrete Foundation with expansion anchor bolt, appropriate for 400 W Modules	Array	4	994,492.69	3,977,970.75
1.12	Galvanized Pipe, 6 Inch	m	120	3,683.31	441,996.75
1.13	Termination Kit (Waterproof joining cable) suitable for 3 core, 95mm cable	Pcs	1 PCS	16,200.00	16,200.00
1.14	Stainless Steel Safety Cable with accessories, 12mm, 95 Mtr double rope	SET	2 SET	51,566.29	103,132.58
1.15	Proper Lightning Arrestor System	SET	1 SET	220,998.38	220,998.38
1.16	Proper grounding system Earthling rod C/W Clamp with 6 mm Grounding Cable	SET	1 SET	198,898.54	198,898.54
1.17	Well head base plate with pump handling ring	SET	1 SET	132,599.03	132,599.03
1.18	Water Flaw Meter with fitting accessories	Pcs	1 PCS	272,564.66	272,564.66
1.19	Civil works: Ground clearance, Equipment house, and concrete	LS	ls	-	

	foundation as per the Design, BOQ, Structural & Architectural Drawing				
1.2	Over all system efficiency testing with measurement (Current, Voltage, Flow rate and Pressure), and Approved report preparation with 3 copies.	Ls	1	906,660.00	906,660.00
	Sub Total Birr			-	**19,213,648.91**

Appendix B2: PV system annual operating expenditure, OpEx

Discount rate (d): 7%

Total PW= I + ∑ Cr*[1/(1+d)^N]

Year (N)	Capital cost (Br)	O&M cost (Br)	Replacement cost (Br)	Discount factor	PV Present worth (Br)
0	6,077,455			1	6,077,455
1		7200		0.93	6,696
2		7200		0.86	6,192
3		7200		0.79	5,688
4		7200		0.72	5,184
5		7200		0.65	4,680
6		7200		0.58	4,176
7		7200		0.51	3,672
8		7200		0.44	3,168
9		7200		0.37	2,664
10		7200		0.3	2,160
11		7200		0.23	1,656
12		7200		0.16	1,152
13		7200	2,175,984	0.09	196,486
14		7200		0.02	144

15	7200	-0.05	-360
16	7200	-0.12	-864
17	7200	-0.19	-1,368
18	7200	-0.26	-1,872
19	7200	-0.33	-2,376
20	7200	-0.4	-2,880
21	7200	-0.47	-3,384
22	7200	-0.54	-3,888
23	7200	-0.61	-4,392
24	7200	-0.68	-4,896
25	7200	-0.75	-5,400
		Total PW:	6,289,493

Appendix B_3: Operational Expenditure

Year (N)	O&M cost (Br)	Replacement cost (Br)	Discount factor	OpEx (Br)
0	0		1	0
1	7200		0.93	6,696
2	7200		0.86	6,192
3	7200		0.79	5,688
4	7200		0.72	5,184
5	7200		0.65	4,680
6	7200		0.58	4,176
7	7200		0.51	3,672
8	7200		0.44	3,168
9	7200		0.37	2,664
10	7200		0.3	2,160
11	7200		0.23	1,656
12	7200		0.16	1,152
13	7200	2,175,984	0.09	196,486
14	7200		0.02	144
15	7200		-0.05	-360
16	7200		-0.12	-864
17	7200		-0.19	-1,368
18	7200		-0.26	-1,872
19	7200		-0.33	-2,376
20	7200		-0.4	-2,880
21	7200		-0.47	-3,384
22	7200		-0.54	-3,888
23	7200		-0.61	-4,392
24	7200		-0.68	-4,896
25	7200		-0.75	-5,400

Total PW:	212,038

Appendix C_1: Annual production cost for the wheat crop under full sunlight. Values adapted from [FEWS NET: Ethiopia Price Bulletin, January 31, 2022].

Costs in Br/ha	**Wheat**
Seed	9,010
Fertilizer	32,330
Irrigation total cost	8,745
Total	50,085

Appendix C_2: Crop production cost under full sunlight and under AV partial shading

Crop Production Cost under Full Sunlight (Br/ha)	**Irrigation Water Saving (%)**	**Crop Production Cost under AV Partial Shading (Br/ha)**
50,085	11.5[a]	50,085

[a] *Due to scarcity of bibliographic data on water saving for some crops under shade, they are assigned the mean between 14% and 9%*

Appendix D: Selected wheat type

Common Name(s)	Common wheat, bread wheat
Scientific Name	*Triticum aestivum*
Days to Harvest	Spring wheat 120 days, Winter wheat 240 days
Light	Full and partial sun
Water	Low water
Soil	Well-drained loamy soil
Fertilizer	1- 2-1 NPK or compost
Pests	Aphids, armyworms, and stinkbugs
Diseases	Bacterial leaf streak, basal glume rot, ergot, powdery mildew, rusts, and wheat mosaic

Appendix E: Irrigation methods and its applicability to solar pumps.

Irrigation method	Typical application efficiency	Typical head	Solar pump applicability
Open Channels	50-60%	0.5-1m	Yes
Sprinkler	70%	10-20m	No
drip	85%	1-2m	Yes
Flood	40-50%	**121**	**+13**